Magnetic excitations in rare-earth antiferromagnets with bilinear and biquadratic pair couplings: Application to DySb

M. J. Sablik
Fairleigh Dickinson University, Teaneck, New Jersey 07666

Y. L. Wang
Florida State University, Tallahassee, Florida 32306

(Received 11 October 1978)

A Green's-function formalism is constructed for the purpose of computing the elementary excitation energies in a type-II antiferromagnet with Heisenberg exchange and quadrupolar couplings in a cubic crystal field. Three types of excitation modes are found: a longitudinal mode (L mode) associated with O_0^1 and O_0^2 operators ($\Delta m = 0$), a transverse mode ($T1$ mode) associated with $O_{\pm 1}^1$ and $O_{\pm 1}^2$ operators ($\Delta m = \pm 1$), and a second transverse mode ($T2$ mode) associated with $O_{\pm 2}^2$ operators ($\Delta m = \pm 2$). In the ordered phase the L-mode and $T1$-mode excitations are mixed magnetic dipolar and quadrupolar excitations. In the disordered phase, as a consequence of cubic symmetry, the magnetic dipolar modes decouple from the quadrupolar modes, giving rise to the possibility of observing a pure quadrupolar excitation. Cubic symmetry also demands that in the disordered phase certain of the excitation energies in the L, $T1$, and $T2$ modes have identical dispersion curves. In general, the dispersion in both the ordered and disordered phase is complicated owing to the inclusion of next-nearest-neighbor coupling. The theory is applied to DySb, a type-II antiferromagnet with strong evidences of quadrupolar coupling.

I. INTRODUCTION

Knowledge of collective excitations in a many-body system is crucial in the understanding of the behavior of the system. In a simple magnetic system, described by the Heisenberg Hamiltonian, spin waves[1] are the elementary excitations as observed in many of the transition-metal compounds. The neutron-inelastic-scattering technique[2] has been used to measure the dispersions, the temperature dependence, and the damping of the spin waves. Measurements of the various thermodynamic quantities also point to (while less directly) the existence of the spin waves. In rare earths the picture is generally greatly complicated by the effects of the crystal field.[3] Indeed, even for a simple ferromagnetic ordering, the elementary spin-wave picture of excitation by creating a spin deviation from the ordered state may no longer be a valid description. Furthermore, because of the existence of splittings in the single-ion energy level (due to the crystal-field interaction) even in the absence of a magnetic ordering, well-defined collective excitation modes can be found.[4] The extensive research, both experimental and theoretical, on the induced-moment singlet-ground-state systems has unraveled much of the mystery of such excitations, and the term magnetic excitons has often been used.[4] In parallel to this development, collective excitations in higher multipolar coupled systems have aroused a great deal of attention and much work has been devoted to their research, especially for systems with quadrupolar pair couplings.[5,6] The motivation was the realizing of the prevalence of quadrupolar couplings in many a rare-earth system. Many striking phenomena have been attributed to the effects of quadrupolar pair coupling. For example, it drives a continuous second-order phase transition to a discontinuous first-order phase transition[7]; it produces a cooperative Jahn-Teller phase transition.[8]

Theoretical considerations on the quadrupolar pair coupled systems have, however, been limited to the simple spin-one model[6] until very recently. Sablik and Wang[9] briefly discussed the effects of crystal field in a ferromagnet model. Similar to the case of a Heisenberg (bilinear pair) coupling in the presence of crystal-field splittings in a single-ion energy level, excitations produced by the quadrupolar pair couplings can exist in the absence of a magnetic ordering as well as in the magnetically ordered phase. In a crystal-field system with the Heisenberg couplings, magnetic excitations have been observed both above and below the magnetic-ordering temperature with little damping even at temperatures appreciably higher than the ordering temperature. In certain systems a soft mode is associated with the order-disorder transition[10]; in others a divergence in the in-

tensity of the central mode is responsible.[11] No neutron work has been performed on systems with quadrupolar pair couplings. One of the purposes for writing this paper is, indeed, to promote such experimental works.

We shall consider DySb as the specific compound in our discussion, because DySb is one of the rare-earth compounds displaying the effects of quadrupolar pair couplings and because there is a growing number of experimental papers on this compound.[7,12] The formalism developed here is, however, more general and can be used for other systems with complicated crystal-field energy-level schemes and general multiple pair couplings. In view of the fact that DySb is a type-II fcc antiferromagnet,[12] we develop a formalism for a general antiferromagnet separable into two sublattices. Lines[13] has calculated the antiferromagnetic spin-wave energies for the two-sublattice Heisenberg antiferromagnets. Our calculation, which includes the crystal-field potential and the quadrupolar pair couplings, obviously becomes much more involved. We nonetheless show a systematic approach of obtaining the RPA Green's-function results.

While presenting the specific results for DySb, we also emphasize on one hand the effects of crystal field on the quadrupolar pair coupled systems, and on the other hand the effects of quadrupolar pair couplings on systems with crystal-field splittings and only bilinear couplings. We show in general that for a magnetic system of cubic symmetry, the excitation modes can be classified into three categories—one longitudinal type and two transverse types. While in the ordered phase the excitations are created by the linear combination of dipolar and quadrupolar operators, in the paramagnetic phase they are pure dipolar or quadrupolar in character. The calculation for the fcc type-II antiferromagnet performed here not only yields the excitation spectrum of a real physical system like DySb, it also lays the ground work for determining how the competition between nearest-neighbor and next-nearest-neighbor bilinear and biquadratic couplings is responsible for stabilizing various types of ordering. This latter problem, however, will not be elaborated in this paper.

The organization of this paper is as follows. We present a model Hamiltonian for a type-II antiferromagnet, taking into account the crystal-field potential and bilinear and biquadratic couplings. We then present the Green's-function formalism used to obtain the excitation energies. We illustrate our procedure by first showing how the simpler case of the ferromagnet is treated. We then extend the formalism to a type-II antiferromagnet. The effect of cubic symmetry on excitations in the paramagnet is discussed. Finally, the formalism is applied specifically to DySb, for which we present numerically computed results. Our discussion and conclusion summarize our principal findings.

II. THE HAMILTONIAN

In order to discuss an fcc rare-earth system with antiferromagnetic ordering such as DySb, we have to consider next-nearest-neighbor (nnn) interactions as well as nearest-neighbor (nn) interactions.[14] For an fcc type-II ordering and, indeed, for type I as well, we can consider up spins to be on one sublattice (say, A) and down spins to be on another sublattice (say, B). An appropriate Hamiltonian, which includes both bilinear and biquadratic couplings, would then be

$$
\begin{aligned}
H = \sum_{i}^{A} V_c(i,A) + \sum_{i}^{B} V_c(i,B) - \Bigg[& \sum_{\langle ii' \rangle}^{AA} \sum_{Q=-1}^{1} (-)^Q \hat{J}_{(p)} O_Q^1(i,A) O_{-Q}^1(i',A) \\
& + \sum_{\langle ij \rangle}^{AB} \sum_{Q=-1}^{1} (-)^Q \hat{J}_{(a)} [O_Q^1(i,A) O_{-Q}^1(j,B) + O_Q^1(j,B) O_{-Q}^1(1,A)] \\
& + \sum_{\langle jj' \rangle}^{BB} \sum_{Q=-1}^{1} (-)^Q \hat{J}_{(p)} O_Q^1(j,B) O_{-Q}^1(j',B) \Bigg] \\
- \sum_{\langle\langle ij \rangle\rangle}^{AB} \sum_{Q=-1}^{1} & (-)^Q \hat{I}_{(a)} [O_Q^1(i,A) O_{-Q}^1(j,B) + O_Q^1(j,B) O_{-Q}^1(i,A)] \\
- \Bigg[& \sum_{\langle ii' \rangle}^{AA} \sum_{Q=-2}^{2} (-)^Q \hat{K}_{(p)} O_Q^2(i,A) O_{-Q}^2(i',A) \\
& + \sum_{\langle ij \rangle}^{AB} \sum_{Q=-2}^{2} (-)^Q \hat{K}_{(a)} [O_Q^2(i,A) O_{-Q}^2(j,B) + O_Q^2(j,B) O_{-Q}^2(i,A)] + \sum_{\langle jj' \rangle}^{BB} \sum_{Q=-2}^{2} (-)^Q \hat{K}_{(p)} O_Q^2(j,B) O_{-Q}^2(j',B) \Bigg] \\
- \sum_{\langle\langle ij \rangle\rangle}^{AB} \sum_{Q=-2}^{2} & (-)^Q \hat{L}_{(a)} [O_Q^2(i,A) O_{-Q}^2(j,B) + O_Q^2(j,B) O_{-Q}^2(i,A)] \ . \qquad (1)
\end{aligned}
$$

A sum over AB and $\langle\langle ij\rangle\rangle$, for example, denotes a sum over next-nearest-neighbor pairs of ions, one on the A sublattice and one on the B sublattice; whereas a sum over BB and $\langle jj'\rangle$ denotes a sum over nearest-neighbor pairs of ions, both on the B sublattice. In a type-II antiferromagnetic ordering, there are *no* next-nearest-neighbor pairs that are parallel,[14] and hence the absence of sums over AA and $\langle\langle ii'\rangle\rangle$ and sums over BB and $\langle\langle jj'\rangle\rangle$. The single-ion term $V_c(i,A)$ represents the cubic crystal-field potential at a site i on the A sublattice and, following Lea, Leask, and Wolf,[15] is given by

$$V_c(i,A)=B_4[O_0^4(i,A)+5O_4^4(i,A)]+B_6[O_0^6(i,A)-21O_4^6(i,A)] \ . \tag{2}$$

The operators O_m^n are spherical tensor operators of order n, properly normalized. These operators may be written in terms of angular-momentum operators and expressions for them may be found in various texts.[16] For convenience, we list the following few:

$$\begin{aligned} O_0^1 &= J_z \\ O_{\pm 1}^1 &= \mp(\tfrac{1}{2})^{1/2} J_\pm \\ O_0^2 &= 3J_z^2 - J(J+1) \\ O_{\pm 1}^2 &= \mp 6^{1/2}\tfrac{1}{2}(J_z J_\pm + J_\pm J_z) \\ O_{\pm 2}^2 &= (\tfrac{3}{2})^{1/2} J_\pm J_\pm \ . \end{aligned} \tag{3}$$

In Eq. (1) the coupling energies are assumed to be isotropic, i.e., the same for all components Q. Couplings are distinguished only by whether the spins of the ions are parallel (p) or antiparallel (a), and whether the ions are nearest neighbors or next-nearest neighbors. The energies $\hat{J}_{(p)}$ and $\hat{I}_{(p)}$ are associated with exchange (bilinear) coupling between parallel spins and the energies $\hat{K}_{(a)}$ and $\hat{L}_{(a)}$ are associated with quadrupolar (biquadratic) coupling between antiparallel spins.

Our procedure now is to split the Hamiltonian into two parts, the mean-field Hamiltonian and the perturbation describing the correlation of fluctuations from the mean field. Assuming that the system orders along the z axis, we obtain

$$\begin{aligned} H_0 = \sum_i^A [& V_c(i,A) - 2z_{(p)}\hat{J}_{(p)}\langle O_0^1(A)\rangle O_0^1(i,A) - 2z_{(a)}\hat{J}_{(a)}\langle O_0^1(B)\rangle O_0^1(i,A) \\ & - 2z_{(p)}\hat{K}_{(p)}\langle O_0^2(A)\rangle O_0^2(i,A) - 2z_{(a)}\hat{K}_{(a)}\langle O_0^2(B)\rangle O_0^2(i,A) \\ & - 2y_{(a)}\hat{I}_{(a)}\langle O_0^1(B)\rangle O_0^1(i,A) - 2y_{(a)}\hat{L}_{(a)}\langle O_0^2(B)\rangle O_0^2(i,A)] \\ + \sum_i^B [& V_c(i,B) - 2z_{(p)}\hat{J}_{(p)}\langle O_0^1(B)\rangle O_0^1(i,B) - 2z_{(a)}\hat{J}_{(a)}\langle O_0^1(A)\rangle O_0^1(i,B) \\ & - 2z_{(p)}\hat{K}_{(p)}\langle O_0^2(B)\rangle O_0^2(i,B) - 2z_{(a)}\hat{K}_{(a)}\langle O_0^2(A)\rangle O_0^2(i,B) \\ & - 2y_{(a)}\hat{I}_{(a)}\langle O_0^1(A)\rangle O_0^1(i,B) - 2y_{(a)}\hat{L}_{(a)}\langle O_0^2(A)\rangle O_0^2(i,B)] \ , \end{aligned} \tag{4}$$

and

$$H_{\text{int}} = H - H_0 \ . \tag{5}$$

In Eq. (4), $z_{(p)}$, $z_{(a)}$, $y_{(p)}$, and $y_{(a)}$ are the nn and nnn coordination numbers associated with parallel and antiparallel magnetic moments, respectively. The mean-field Hamiltonian, consisting entirely of single-ion terms, can then be diagonalized in the self-consistent fields $\langle O_0^1(A)\rangle$, $\langle O_0^1(B)\rangle$, $\langle O_0^2(A)\rangle$, and $\langle O_0^2(B)\rangle$. In this way, the molecular-field energy levels and molecular-field eigenstates can be obtained for each rare-earth ion in the system. These will then be used as basis states for the Green's-function calculation below.

III. NONINTERACTING GREEN'S FUNCTIONS

We define a noninteracting Green's function

$$g(O_Q^K, O_{Q'}^{K'}) \equiv \{ \langle T_\tau [O_Q^K(i,\tau) - \langle O_Q^K\rangle] \times [O_{Q'}^{K'}(j,0) - \langle O_{Q'}^{K'}\rangle]\rangle_0 \}_{\vec{q},\omega_l} \ , \tag{6}$$

where T_τ is the usual τ-ordering operator[17] and where $O_Q^K(\tau) = e^{H_0\tau} O_Q^K e^{-H_0\tau}$ is written in the interaction representation. The angular brackets with subscript 0 denote the canonical thermal average with respect to H_0, and the subscripts on the curly brackets denote the $\vec{q}$, ω_l Fourier transformation of the quantity.

To evaluate this noninteracting Green's function, we use standard basis operators.[18,19] These are defined as

$$L_{mn} = |m\rangle\langle n| \quad . \tag{7}$$

The operator L_{mn} transfers an ion from state $|m\rangle$ to state $|n\rangle$, and it should be self-evident that

$$L_{mm'}L_{nn'} = \delta_{m'n}L_{mn'} \quad ,$$

$$[L_{mm'}, L_{nn'}] = \delta_{m'n}L_{mn'} - \delta_{mn'}L_{nm'} \quad .$$

The ensemble average D_n of the operator L_{nn} measures the probability that state n is occupied. $D_n \equiv e^{-\beta E_n}/Z$, where $Z \equiv \sum_m e^{-\beta E_m}$, and where $e^{-\beta E_n}$ is the Boltzmann factor associated with level n. We express the operator $O_Q^K(i)$ in terms of standard basis operators at site i as follows:

$$O_Q^K(i) = \sum_{m,n} \langle m|O_Q^K|n\rangle L_{mn}^i \quad . \tag{8}$$

Written in terms of standard basis operators, our noninteracting Green's function takes the form

$$g(O_Q^K, O_{Q'}^{K'}) = \sum_{\substack{n,m \\ r,s}} \langle m|O_Q^K - \langle O_Q^K\rangle|n\rangle\langle r|O_{Q'}^{K'} - \langle O_{Q'}^{K'}\rangle|s\rangle \{\langle T_\tau L_{mn}^i(\tau) L_{rs}^j(0)\rangle_0\}_{\vec{q},\omega_l} \quad , \tag{9}$$

where the standard basis operator Green's function

$$\langle T_\tau L_{mn}^i(\tau) L_{rs}^j(0)\rangle_0 = \begin{cases} \dfrac{1}{Z}\mathrm{Tr}\, e^{-\beta H_0} L_{mn}^i(\tau) L_{rs}^j(0) \ , & \tau > 0 \\ \dfrac{1}{Z}\mathrm{Tr}\, e^{-\beta H_0} L_{rs}^j(0) L_{mn}^i(\tau) \ , & \tau < 0 \ . \end{cases} \tag{10}$$

Here Z is the partition function associated with the molecular-field Hamiltonian H_0. Following Yang and Wang,[19] we evaluate Eq. (10) as follows:

$$\frac{1}{Z}\mathrm{Tr}\, e^{-\beta H_0} L_{mn}^i(\tau) L_{rs}^j(0) = \frac{1}{Z} e^{+\epsilon_{mn}\tau} \sum_p e^{-\beta\epsilon_p} \langle p|L_{mn}^i L_{rs}^i|p\rangle \delta_{ij}$$

$$= \frac{1}{Z} e^{+\epsilon_{mn}\tau} e^{-\beta\epsilon_s} \langle s|L_{mn}^i|r\rangle \delta_{ij} = D_m \delta_{ij}\delta_{ms}\delta_{rn} e^{+\epsilon_{mn}\tau} \quad ,$$

and similarly

$$\frac{1}{Z}\mathrm{Tr}\, e^{-\beta H_0} L_{rs}^j(0) L_{mn}^i(\tau) = D_n \delta_{ij}\delta_{ms}\delta_{rn} e^{+\epsilon_{mn}\tau} \quad ,$$

where we have written $\epsilon_{mn} = \epsilon_m - \epsilon_n$. The Fourier transformation in τ is defined as follows[17]:

$$G(\tau) = \sum_n e^{-i\omega_n\tau} G(\omega_n) \quad ,$$

$$\omega_n = 2n\pi/\beta \ , \quad \beta = 1/k_B T \quad , \tag{11}$$

so

$$G(\omega_n) = \frac{1}{2\beta}\int_{-\beta}^{\beta} G(\tau) e^{i\omega_n\tau} d\tau \ ; \tag{12}$$

and after denoting $D_{nm} = D_n - D_m$, we obtain

$$\{\langle T_\tau L_{mn}^i(\tau) L_{rs}^j(0)\rangle_0\}_{\vec{q},\omega_l} = \frac{D_{nm}\delta_{rn}\delta_{ms}}{\beta(\epsilon_{mn} + i\omega_l)} \quad , \tag{13}$$

provided $\epsilon_{mn} \neq 0$. In the case where $m \neq n$ but $\epsilon_m = \epsilon_n$, Eq. (13) yields zero on the right-hand side except when $\omega_l = 0$, in which case $D_{nm}/\beta\epsilon_{mn} \to D_n$ in the limit of $\epsilon_{mn} \to 0$, as can be seen by using L'Hôpital's rule. We therefore find Eq. (13) equal to $D_n\delta_{rn}\delta_{ms}\delta(\omega_l)$, where $\delta(\omega_l)$ is 1 if $\omega_l = 0$ and zero otherwise. In the case where $m = n$, we have $L_{mm}^i(\tau) = L_{mm}^i(0)$, and hence we obtain

$$\langle T_\tau L_{mm}^i(\tau) L_{rs}^j(0)\rangle_0 = \langle L_{mm}^i L_{rs}^j\rangle_0 = D_m\delta_{ms}\delta_{rm}\delta_{ij} \quad .$$

The Fourier transform then produces

$$\{\langle T_\tau L_{mm}^i(\tau) L_{rs}^j(0)\rangle_0\}_{\vec{q},\omega_l} = D_m\delta_{ms}\delta_{rm}\delta(\omega_l) \quad . \tag{14}$$

Using these results, we thus see that

$$g(O_Q^K, O_{Q'}^{K'}) = \sum_{\substack{mn \\ m\neq n}} \langle m|O_Q^K - \langle O_Q^K\rangle|n\rangle\langle n|O_{Q'}^{K'} - \langle O_{Q'}^{K'}\rangle|m\rangle \frac{D_{nm}}{\beta(\epsilon_{mn} + i\omega_l)}$$

$$+ \sum_{\substack{m,n \\ \epsilon_m = \epsilon_n}} \langle m|O_Q^K - \langle O_Q^K\rangle|n\rangle\langle n|O_{Q'}^{K'} - \langle O_{Q'}^{K'}\rangle|m\rangle D_n\delta(\omega_l) \quad . \tag{15}$$

Because there is no interion interaction in the unperturbed Hamiltonian H_0 with respect to which $g(O_Q^K, O_{Q'}^{K'})$ is defined, we note that $g(O_Q^K, O_{Q'}^{K'})$ is $\vec{q}$ independent. Also, we note that in cubic symmetry the products $\langle m|O_Q^K|n\rangle\langle n|O_{Q'}^{K'}|m\rangle$ can be nonzero only if $Q=-Q'$, unless $K=K'=2$, where $Q=Q'=2$ is also possible. Thus, only $g(O_{Q'}^K, O_{-Q}^{K'})$, $g(O_2^2, O_2^2)$ and $g(O_{-2}^2, O_{-2}^2)$ will occur in our calculation.

Buyers *et al.*[20] have evaluated the functions $g(O_Q^1, O_{-Q}^1)$ and have obtained somewhat similar results using an equation-of-motion type of derivation. However, they did not obtain the second term. This term can be omitted in the calculation of excitation energies, but should be included in order to find the Green's functions correctly. It will be important, for example, to include it in calculating the contribution to the central mode in neutron-scattering measurements.

Now that we have obtained an expression for $g(O_Q^K, O_{Q'}^{K'})$, standard basis operators disappear from the formalism. An alternate approach would be to compute Green's functions of standard basis operators evaluated with respect to the full Hamiltonian H.[18,19,21] For systems with biquadratic coupling and many crystal-field levels, an unwieldy number of Green's functions would have to be evaluated and combined in order to obtain correlation functions of the O_Q^K operators. The procedure we are about to present next thus represents a great simplification and should be preferred over those methods which explicitly use the standard basis operators.

IV. RPA GREEN'S FUNCTIONS FOR A MODEL FERROMAGNET IN CUBIC SYMMETRY

In a previous paper[9] we have briefly discussed the formulation of Green's functions in the random-phase approximation (RPA) for a model ferromagnet in cubic symmetry with bilinear and biquadratic coupling. We here present more complete details of that formulation. This should serve as an introduction to the method we shall later develop for treatment of a type-II antiferromagnet.

We wish to evaluate

$$G(O_Q^K, O_{Q'}^{K'}) \equiv \langle T_\tau[O_Q^K(i,\tau) - \langle O_Q^K\rangle][O_{Q'}^{K'}(j,0) - \langle O_{Q'}^{K'}\rangle]\rangle_{\vec{q},\omega_l} \ , \tag{16}$$

where this time the angular brackets denote a canonical ensemble average with respect to the full Hamiltonian H and the operators in the Green's function are in the Heisenberg representation. Following Abrikosov *et al.*,[17] we expand the Green's function in the form

$$G(O_Q^K, O_{Q'}^{K'}) = \{\langle T_\tau[O_Q^K(i,\tau) - \langle O_Q^K\rangle][O_{Q'}^{K'}(j,0) - \langle O_{Q'}^{K'}\rangle]S(\beta)\rangle_0 / \langle S(\beta)\rangle_0\}_{\vec{q},\omega_l} \tag{17}$$

where the S matrix $S(\beta)$ is defined as

$$S(\beta) = 1 + \sum_{n=1}^{\infty} \frac{(-1)^n}{n!} \int_0^\beta \cdots \int_0^\beta T_\tau[H_{\rm int}(\tau_1) H_{\rm int}(\tau_2) \cdots] d\tau_1 \cdots d\tau_n \ . \tag{18}$$

In Eq. (17), the operators on the right-hand side are in the interaction representation.

Equation (17) consists of an infinite series of terms, each of which can be represented by a diagram. The approximation generally used consists in selecting a set of diagrams which represent the largest contribution to the sum of terms. In a system of localized magnetic ions the reciprocal of the effective number of ions interacting with a given ion has been used as an expansion parameter.[22] This is known as the $1/z$ expansion. The leading order terms are chainlike diagrams. Selecting only these diagrams gives the approximation known as the chain approximation, equivalent to RPA.

In our case, the sum of chainlike diagrams may be represented algebraically in terms of "bare" interactions as follows:

$$G(O_Q^K, O_{Q'}^{K'}) = g(O_Q^K, O_{Q'}^{K'}) + \sum_{K_1=1}^{2} \sum_{Q_1=-K_1}^{K_1} g(O_Q^K, O_{Q_1}^{K_1}) \mathcal{J}_{K_1 Q_1}(\vec{q}) G(O_{-Q_1}^{K_1}, O_{Q'}^{K'}) \ , \tag{19}$$

where the bare interaction $\mathcal{J}_{K_1 Q_1}(\vec{q})$ is given as

$$\mathcal{J}_{K_1 Q_1}(\vec{q}) \equiv J_{Q_1}(\vec{q})\delta_{K_1 1} + K_{Q_1}(\vec{q})\delta_{K_1 2} \ , \tag{20}$$

and where

$$J_0(\vec{q}) = 2\beta\hat{J}(\vec{q}) \ , \quad K_0(\vec{q}) = 2\beta\hat{K}(\vec{q}) \ ,$$
$$J_1(\vec{q}) = -2\beta\hat{J}(\vec{q}) \ , \quad K_1(\vec{q}) = -2\beta\hat{K}(\vec{q}) \ , \tag{21}$$
$$K_2(\vec{q}) = 2\beta\hat{K}(\vec{q}) \ .$$

The functions $\hat{J}(\vec{q})$ and $\hat{K}(\vec{q})$ are the Fourier transforms

$$\hat{J}(\vec{q}) = z\hat{J}\left(\frac{1}{z}\sum_{\vec{\delta}} e^{i\vec{q}\cdot\vec{\delta}}\right) \equiv z\hat{J}\gamma_0(\vec{q}) \ ,$$
$$\hat{K}(\vec{q}) = z\hat{K}\left(\frac{1}{z}\sum_{\vec{\delta}} e^{i\vec{q}\cdot\vec{\delta}}\right) \equiv z\hat{K}\gamma_0(\vec{q}) \ , \tag{22}$$

where only vectors $\vec{\delta}$ to near-neighbor sites enter the transform if we adopt the nearest-neighbor interaction model.

Equation (19) gives rise to several coupled sets of equations. There is one set for longitudinal interactions ($Q=0$), one set for transverse interactions that result in a raising and lowering of spin projection by one ($\Delta m_J = \pm 1$), and another set for transverse interactions resulting in raisings and lowerings by two ($\Delta m_J = \pm 2$). We shall take each set in turn.

In the longitudinal case, we have

$$G_{00} = g_{00} + g_{00}J_0(\vec{q})G_{00} + g_{0x}K_0(\vec{q})G_{x0} \ , \tag{23a}$$
$$G_{x0} = g_{x0} + g_{x0}J_0(\vec{q})G_{00} + g_{xx}K_0(\vec{q})G_{x0} \ , \tag{23b}$$
$$G_{0x} = g_{0x} + g_{00}J_0(\vec{q})G_{0x} + g_{0x}K_0(\vec{q})G_{xx} \ , \tag{23c}$$
$$G_{xx} = g_{xx} + g_{x0}J_0(\vec{q})G_{0x} + g_{xx}K_0(\vec{q})G_{xx} \ , \tag{23d}$$

where we have shortened the notation by writing

$$\begin{aligned} &G_{00} \equiv G(O_0^1, O_0^1) \ , \quad g_{00} \equiv g(O_0^1, O_0^1) \ , \\ &G_{x0} \equiv G(O_0^2, O_0^1) \ , \quad g_{x0} \equiv g(O_0^2, O_0^1) \ , \\ &G_{0x} \equiv G(O_0^1, O_0^2) \ , \quad g_{0x} \equiv g(O_0^1, O_0^2) \ , \\ &G_{xx} \equiv G(O_0^2, O_0^2) \ , \quad g_{xx} \equiv g(O_0^2, O_0^2) \ . \end{aligned} \tag{24}$$

Diagrams representing Eqs. (23) may be seen in Fig. 1.

The first two equations in the set (23) may be solved separately from the second two, yielding the solutions

$$\begin{aligned} &G_{00} = [g_{00} - (g_{00}g_{xx} - g_{0x}g_{x0})K_0(\vec{q})]/D_0 \ , \\ &G_{x0} = g_{x0}/D_0 \ , \\ &G_{0x} = g_{0x}/D_0 \ , \\ &G_{xx} = [g_{xx} - (g_{00}g_{xx} - g_{0x}g_{x0})J_0(\vec{q})]/D_0 \ , \end{aligned} \tag{25}$$

where, returning to our original notation, we have

$$\begin{aligned} D_0 = D_0(\vec{q}, \omega_l) = &[1 - g(O_0^1, O_0^1)J_0(\vec{q})] \\ &\times [1 - g(O_0^2, O_0^2)K_0(\vec{q})] \\ &- g(O_0^1, O_0^2)g(O_0^2, O_0^1) \\ &\times J_0(\vec{q})K_0(\vec{q}) \ . \end{aligned} \tag{26}$$

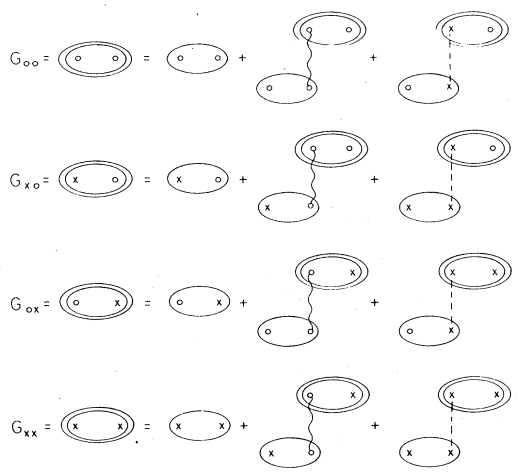

FIG. 1. Chain diagrams for the longitudinal Green's functions in the nn ferromagnet model using bare interactions. The wiggly lines refer to $J_0(\vec{q})$; the dashed lines to $K_0(\vec{q})$. The vertices enclosed with a single ellipse represent $g(O_0^K, O_0^{K'})$ functions. x is an O_0^2 vertex; 0 is an O_0^1 vertex.

The g functions are, of course, functions of ω_l.

The transverse $\Delta m = \pm 1$ case is similar. Instead of Eqs. (24), we shall use the replacement

$$\begin{aligned} &G_{00} = G(O_1^1, O_{-1}^1) \ , \quad g_{00} = g(O_1^1, O_{-1}^1) \ , \\ &G_{x0} = G(O_1^2, O_{-1}^1) \ , \quad g_{x0} = g(O_1^2, O_{-1}^1) \ , \\ &G_{0x} = G(O_1^1, O_{-1}^2) \ , \quad g_{0x} = g(O_1^1, O_{-1}^2) \ , \\ &G_{xx} = G(O_1^2, O_{-1}^2) \ , \quad g_{xx} = g(O_1^2, O_{-1}^2) \ . \end{aligned} \tag{27}$$

The solutions to the resulting chain equations are then the same as Eqs. (25), but with the replacement $J_0(\vec{q})$ by $J_1(\vec{q})$, $K_0(\vec{q})$ by $K_1(\vec{q})$, and D_0 by D_1, where

$$\begin{aligned} D_1 = D_1(\vec{q}, \omega_l) = &[1 - g(O_1^1, O_{-1}^1)J_1(\vec{q})] \\ &\times [1 - g(O_1^2, O_{-1}^2)K_1(\vec{q})] \\ &- g(O_1^1, O_{-1}^2)g(O_1^2, O_{-1}^1) \\ &\times J_1(\vec{q})K_1(\vec{q}) \ . \end{aligned} \tag{28}$$

The transverse $\Delta m = \pm 2$ case is slightly different in that there is only one interaction to consider, namely $K_2(\vec{q})$. However, for cubic symmetry the functions $g(O_2^2, O_2^2)$ and $g(O_{-2}^2, O_{-2}^2)$ are nonzero and therefore enter the chain equations. Our chain equations become

$$G(O_2^2,O_{-2}^2)=g(O_2^2,O_{-2}^2)+g(O_2^2,O_{-2}^2)K_2(\vec{q})G(O_2^2,O_{-2}^2)+g(O_2^2,O_2^2)K_2(\vec{q})G(O_{-2}^2,O_{-2}^2)\ ,$$
$$G(O_{-2}^2,O_{-2}^2)=g(O_{-2}^2,O_{-2}^2)+g(O_{-2}^2,O_{-2}^2)K_2(\vec{q})G(O_2^2,O_{-2}^2)+g(O_{-2}^2,O_2^2)K_2(\vec{q})G(O_{-2}^2,O_{-2}^2)\ ,$$
$$G(O_{-2}^2,O_2^2)=g(O_{-2}^2,O_2^2)+g(O_{-2}^2,O_{-2}^2)K_2(\vec{q})G(O_2^2,O_2^2)+g(O_{-2}^2,O_2^2)K_2(\vec{q})G(O_{-2}^2,O_2^2)\ ,$$
$$G(O_2^2,O_2^2)=g(O_2^2,O_2^2)+g(O_2^2,O_{-2}^2)K_2(\vec{q})G(O_2^2,O_2^2)+g(O_2^2,O_2^2)K_2(\vec{q})G(O_{-2}^2,O_2^2)\ , \tag{29}$$

and these yield the solutions

$$G(O_2^2,O_{-2}^2)=\{g(O_2^2,O_{-2}^2)-K_2(\vec{q})[g(O_2^2,O_{-2}^2)g(O_{-2}^2,O_2^2)-g(O_2^2,O_2^2)g(O_{-2}^2,O_{-2}^2)]\}/D_2\ ,$$
$$G(O_{-2}^2,O_2^2)=\{g(O_{-2}^2,O_2^2)-K_2(\vec{q})[g(O_{-2}^2,O_2^2)g(O_2^2,O_{-2}^2)-g(O_{-2}^2,O_{-2}^2)g(O_2^2,O_2^2)]\}/D_2\ ,$$
$$G(O_{-2}^2,O_{-2}^2)=g(O_{-2}^2,O_{-2}^2)/D_2\ ,\quad G(O_2^2,O_2^2)=g(O_2^2,O_2^2)/D_2\ , \tag{30}$$

where

$$D_2=D_2(\vec{q},\omega_l)=[1-K_2(\vec{q})g(O_2^2,O_{-2}^2)][1-K_2(\vec{q})g(O_{-2}^2,O_2^2)]-g(O_2^2,O_2^2)g(O_{-2}^2,O_{-2}^2)[K_2(\vec{q})]^2\ . \tag{31}$$

We thus have obtained the RPA Green's functions for a model nn ferromagnet in cubic symmetry with bilinear and biquadratic coupling. The poles of the Green's functions, analytically continued by replacing $i\omega_l\rightarrow\omega+i0^+$, give the energies of excitations. Namely, the excitation energies are obtained by solving the three equations

$$D_0(\vec{q},\omega)=0\ ,\quad D_1(\vec{q},\omega)=0\ ,\quad D_2(\vec{q},\omega)=0\ , \tag{32}$$

defining longitudinal (L-mode) excitations, transverse $\Delta m=\pm1$ ($T1$-mode) excitations, the transverse $\Delta m=\pm2$ ($T2$-mode) excitations, respectively. It should be noted that the formulation presented in our previous paper[9] is slightly different, using chain equations represented in terms of effective interactions. That is, our chain equation had the form

$$G(O_Q^K,O_{Q'}^{K'})=g(O_Q^K,O_{Q'}^{K'})+\sum_{K_1=1}^{2}\sum_{K_2=1}^{2}\sum_{\eta=-Q,Q}g(O_Q^K,O_\eta^{K_1})\tilde{\mathcal{G}}_{K_1K_2Q}(\vec{q},\omega_l)g(O_{-\eta}^{K_2},O_{Q'}^{K'})\ , \tag{33}$$

where the effective interaction

$$\tilde{\mathcal{G}}_{K_1K_2Q}(\vec{q},\omega_l)=\tilde{\mathcal{G}}_{00}(\vec{q},\omega_l)\delta_{K_11}\delta_{K_21}+\tilde{\mathcal{G}}_{0x}(\vec{q},\omega_l)\delta_{K_11}\delta_{K_22}+\tilde{\mathcal{G}}_{x0}(\vec{q},\omega_l)\delta_{K_12}\delta_{K_21}+\tilde{\mathcal{G}}_{xx}(\vec{q},\omega_l)\delta_{K_12}\delta_{K_22}\ . \tag{34}$$

The functions $\tilde{\mathcal{G}}_{00},\tilde{\mathcal{G}}_{0x},\tilde{\mathcal{G}}_{x0}\tilde{\mathcal{G}}_{xx}$ are displayed diagramatically in Fig. 2. Algebraically, for the longitudinal case, the diagrammatic equations correspond to

$$\tilde{\mathcal{G}}_{00}(\vec{q},\omega_l)=J_0+J_0g_{00}\tilde{\mathcal{G}}_{00}+J_0g_{0x}\frac{K_0}{1-K_0g_{xx}}g_{x0}\tilde{\mathcal{G}}_{00}\ ,$$
$$\tilde{\mathcal{G}}_{xx}(\vec{q},\omega_l)=K_0+K_0g_{xx}\tilde{\mathcal{G}}_{xx}+K_0g_{x0}\frac{J_0}{1-J_0g_{00}}g_{0x}\tilde{\mathcal{G}}_{xx}\ ,$$
$$\tilde{\mathcal{G}}_{0x}(\vec{q},\omega_l)=\left[\frac{J_0}{1-g_{00}J_0}\right]g_{0x}\tilde{\mathcal{G}}_{xx}\ ,$$
$$\tilde{\mathcal{G}}_{x0}(\vec{q},\omega_l)=\tilde{\mathcal{G}}_{xx}g_{x0}\left[\frac{J_0}{1-g_{00}J_0}\right]=\left[\frac{K_0}{1-g_{xx}K_0}\right]g_{x0}\tilde{\mathcal{G}}_{00}\ , \tag{35}$$

the solutions of which are

$$\tilde{\mathcal{G}}_{00}(\vec{q},\omega_l)=J_0(\vec{q})\frac{[1-K_0(\vec{q})g_{xx}(\omega_l)]}{D_0(\vec{q},\omega_l)}\ ,$$
$$\tilde{\mathcal{G}}_{xx}(\vec{q},\omega_l)=K_0(\vec{q})\frac{[1-J_0(\vec{q})g_{00}(\omega_l)]}{D_0(\vec{q},\omega_l)}\ ,$$
$$\tilde{\mathcal{G}}_{0x}(\vec{q},\omega_l)=J_0(\vec{q})\frac{K_0(\vec{q})g_{0x}(\omega_l)}{D_0(\vec{q},\omega_l)}\ ,$$
$$\tilde{\mathcal{G}}_{x0}(\vec{q},\omega_l)=J_0(\vec{q})\frac{K_0(\vec{q})g_{x0}(\omega_l)}{D_0(\vec{q},\omega_l)}\ . \tag{36}$$

Substituting back into Eq. (33) yields the same solutions as before. The advantage of this second approach is that the Green's functions can be obtained without having to first solve simultaneous equations. The disadvantage is that the diagrams are not necessarily obvious. The formulation becomes particularly cumbersome when attempts are made to extend it to the antiferromagnet, and so we have chosen to follow the first approach.

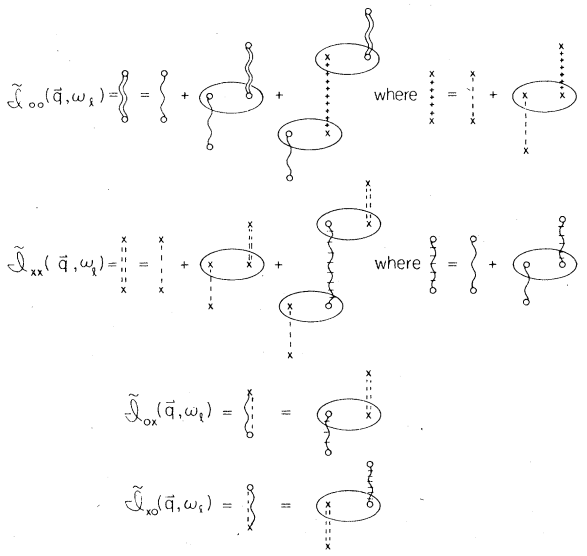

FIG. 2. Diagram equations for the effective interactions in the nn ferromagnet model.

V. RPA GREEN'S FUNCTIONS FOR A TYPE-II ANTIFERROMAGNET

We now generalize the chain approximation to an antiferromagnet with nn and nnn interactions. For type-II ordering, it is essential to consider the nnn interactions.

The general chain equation thus takes the form

$$\begin{aligned} G(a,b) = g(a,b) &+ \sum_{c,d} g(a,c)\, U_{cd}^{(p)} G(d,b) \\ &+ \sum_{c,d} g(a,c)\, U_{c\underline{d}}^{(a)} G(\underline{d},b) \\ &+ \sum_{c,d} g(a,c)\, V_{cd}^{(p)} G(d,b) \\ &+ \sum_{c,d} g(a,c)\, V_{c\underline{d}}^{(a)} G(\underline{d},b) \quad , \end{aligned} \tag{37}$$

where the letters a,b,c,d refer to O_Q^K operators, and where letters that are underlined refer to operators on the "other" sublattice. The U refer to nn interaction energies and the V refer to nnn interaction energies.

In the longitudinal case, we again use our 0 and x notation and let the c,d indices run over $0,x$, where 0 corresponds to an O_0^1 vertex and x corresponds to an O_0^2 vertex. The following relationships hold among the interaction energies.

$$\begin{aligned} &U_{00}^{(p)} = J_0^{(p)}(\vec{q}) \quad , \quad U_{xx}^{(p)} = K_0^{(p)}(\vec{q}) \quad , \\ &U_{0\underline{0}}^{(a)} = J_0^{(a)}(\vec{q}) \quad , \quad U_{x\underline{x}}^{(a)} = K_0^{(a)}(\vec{q}) \quad , \\ &U_{0x}^{(p)} = U_{x0}^{(p)} = U_{0\underline{x}}^{(a)} = U_{x\underline{0}}^{(a)} = 0 \quad , \\ &V_{00}^{(p)} = I_0^{(p)}(\vec{q}) \quad , \quad V_{xx}^{(p)} = L_0^{(p)}(\vec{q}) \quad , \\ &V_{0\underline{0}}^{(a)} = I_0^{(a)}(\vec{q}) \quad , \quad V_{x\underline{x}}^{(a)} = L_0^{(a)}(\vec{q}) \quad , \\ &V_{0x}^{(p)} = V_{x0}^{(p)} = V_{0\underline{x}}^{(a)} = V_{x\underline{0}}^{(a)} = 0 \quad , \end{aligned} \tag{38}$$

where

$$\begin{aligned} J_Q^{(p)}(\vec{q}) &= \eta_Q \beta z_{(p)} \hat{J}_{(p)} \left(\frac{1}{z_{(p)}} \sum_{\langle\delta\rangle}^{AA} e^{i\vec{q}\cdot\vec{\delta}} \right) \\ &= \eta_Q \beta z_{(p)} \hat{J}_{(p)} \gamma_{\mathrm{nn}}^{(p)}(\vec{q}) \quad , \\ K_Q^{(p)}(\vec{q}) &= \eta_Q \beta z_{(p)} \hat{K}_{(p)} \gamma_{\mathrm{nn}}^{(p)}(\vec{q}) \quad , \\ J_Q^{(a)}(\vec{q}) &= \eta_Q \beta z_{(a)} \hat{J}_{(a)} \left(\frac{1}{z_{(a)}} \sum_{\langle\delta\rangle}^{AB} e^{i\vec{q}\cdot\vec{\delta}} \right) \\ &= \eta_Q \beta z_{(a)} \hat{J}_{(a)} \gamma_{\mathrm{nn}}^{(a)}(\vec{q}) \quad , \\ K_Q^{(a)}(\vec{q}) &= \eta_Q \beta z_{(a)} \hat{K}_{(a)} \gamma_{\mathrm{nn}}^{(a)}(\vec{q}) \quad , \\ I_Q^{(p)}(\vec{q}) &= \eta_Q \beta y_{(p)} \hat{I}_{(p)} \left(\frac{1}{y_{(p)}} \sum_{\langle\langle\delta\rangle\rangle}^{AA} e^{i\vec{q}\cdot\vec{\delta}} \right) \\ &= \eta_Q \beta y_{(p)} \hat{I}_{(p)} \gamma_{\mathrm{nnn}}^{(p)}(\vec{q}) \quad , \\ L_Q^{(p)}(\vec{q}) &= \eta_Q \beta y_{(p)} \hat{L}_{(p)} \gamma_{\mathrm{nnn}}^{(p)}(\vec{q}) \quad , \\ I_Q^{(a)}(\vec{q}) &= \eta_Q \beta y_{(a)} \hat{I}_{(a)} \left(\frac{1}{y_{(a)}} \sum_{\langle\langle\delta\rangle\rangle}^{AB} e^{i\vec{q}\cdot\vec{\delta}} \right) \\ &= \eta_Q \beta y_{(a)} \hat{I}_{(a)} \gamma_{\mathrm{nnn}}^{(a)}(\vec{q}) \quad , \\ L_Q^{(a)}(\vec{q}) &= \eta_Q \beta y_{(a)} \hat{L}_{(a)} \gamma_{\mathrm{nnn}}^{(a)}(\vec{q}) \quad . \end{aligned} \tag{39}$$

In these equations $\eta_0 = 2$, $\eta_1 = -2$, and $\eta_2 = 2$, where the factor of 2 arises because we choose to write the Hamiltonian in a symmetrical way [with respect to the two sublattices] as seen in Eq. (1).

If we now examine the set of four equations that result from Eq. (37) for the functions G_{00}, G_{0x}, $G_{0\underline{0}}$, and $G_{x\underline{0}}$, we find that using Kramer's rule, all of these functions have the same denominator, which in particular is a 4×4 determinant, namely,

$$D_0^A(\vec{q},\omega_l) = \begin{vmatrix} g_{00}A_0^{(p)} - 1 & g_{0x}B_0^{(p)} & g_{00}A_0^{(a)} & g_{0x}B_0^{(a)} \\ g_{x0}A_0^{(p)} & g_{xx}B_0^{(p)} - 1 & g_{x0}A_0^{(a)} & g_{xx}B_0^{(a)} \\ g_{0\underline{0}}A_0^{(a)} & g_{0\underline{x}}B_0^{(a)} & g_{0\underline{0}}A_0^{(p)} - 1 & g_{0\underline{x}}B_0^{(p)} \\ g_{x\underline{0}}A_0^{(a)} & g_{x\underline{x}}B_0^{(a)} & g_{x\underline{0}}A_0^{(p)} & g_{x\underline{x}}B_0^{(p)} - 1 \end{vmatrix} \quad . \tag{40}$$

Since 0 and x refer to O_0^1 and O_0^2 vertices respectively, the g functions in this equation are given as follows:

$$\begin{aligned} &g_{00}=g_A(O_0^1,O_0^1)\ ,\quad g_{xx}=g_A(O_0^2,O_0^2)\ ,\\ &g_{0x}=g_{x0}=g_A(O_0^1,O_0^2)\ ,\\ &g_{\underline{00}}=g_B(O_0^1,O_0^1)\ ,\quad g_{\underline{xx}}=g_B(O_0^2,O_0^2)\ ,\\ &g_{0\underline{x}}=g_{\underline{x}0}=g_B(O_0^1,O_0^2)\ , \end{aligned} \tag{41}$$

where subscript A means that in Eq. (15) one employs ϵ_{mn}, D_{nm}, and matrix elements $\langle m|O_Q^K|n\rangle$ and $\langle n|O_{Q'}^{K'}|m\rangle$ which are evaluated by using molecular-field states appropriate to the A sublattice, and subscript B is used similarly for sublattice B. In Eq. (40), we have further consolidated our notation as follows:

$$\begin{aligned} &A_Q^{(p)}(\vec{q})=J_Q^{(p)}(\vec{q})+I_Q^{(p)}(\vec{q})\ ,\\ &A_Q^{(a)}(\vec{q})=J_Q^{(a)}(\vec{q})+I_Q^{(a)}(\vec{q})\ ,\\ &B_Q^{(p)}(\vec{q})=K_Q^{(p)}(\vec{q})+L_Q^{(p)}(\vec{q})\ ,\\ &B_Q^{(a)}(\vec{q})=K_Q^{(a)}(\vec{q})+L_Q^{(a)}(\vec{q})\ . \end{aligned} \tag{42}$$

By setting $D_0^A(\vec{q},\omega_l)=0$, we solve for the poles of the longitudinal Green's functions and hence for the longitudinal excitation energies. $D_0^A(\vec{q},\omega_l)$ may be re-expressed in algebraic form, in which case our equation giving the L-mode excitation energies is

$$\begin{aligned} D_0^A(\vec{q},\omega_l)=&[1-(g_{00}+g_{\underline{00}}A_0^{(p)})[1-(g_{xx}+g_{\underline{xx}})B_0^{(p)}]-(g_{0x}g_{x0}+g_{0\underline{x}}g_{\underline{x}0})A_0^{(p)}B_0^{(p)}\\ &-(g_{0x}g_{\underline{x}0}+g_{x0}g_{0\underline{x}})A_0^{(a)}B_0^{(a)}+g_{00}g_{\underline{00}}[(A_0^{(p)})^2-(A_0^{(a)})^2]\\ &+g_{xx}g_{\underline{xx}}[(B_0^{(p)})^2-(B_0^{(a)})^2]-[(g_{00}g_{xx}-g_{0x}g_{x0})g_{\underline{00}}+(g_{\underline{00}}g_{\underline{xx}}-g_{0\underline{x}}g_{\underline{x}0})g_{00}]\\ &\times[(A_0^{(p)})^2-(A_0^{(a)})^2]B_0^{(p)}-[g_{00}g_{xx}-g_{0x}g_{x0})g_{\underline{xx}}+(g_{\underline{00}}g_{\underline{xx}}-g_{0\underline{x}}g_{\underline{x}0})g_{xx}]\\ &\times[(B_0^{(p)})^2-(B_0^{(a)})^2]A_0^{(p)}+[(g_{00}g_{xx}-g_{0x}g_{x0})(g_{\underline{00}}g_{\underline{xx}}-g_{0\underline{x}}g_{\underline{x}0})]\\ &\times[(A_0^{(p)})^2-(A_0^{(a)})^2][(B_0^{(p)})^2-(B_0^{(a)})^2]=0\ . \end{aligned} \tag{43}$$

This equation appears formidable but actually can be solved numerically for its roots in a straightforward way via the use of a computer.

In the case of the $T1$ mode, Eq. (43) again gives the excitation energies, provided we replace $A_0^{(p)}$ by $A_1^{(p)}$, $B_0^{(p)}$ by $B_1^{(p)}$, $A_0^{(a)}$ by $A_1^{(a)}$, and $B_0^{(a)}$ by $B_1^{(a)}$, and provided we write

$$\begin{aligned} &g_{00}^{(1)}=g_A(O_1^1,O_{-1}^1)\ ,\quad g_{xx}^{(1)}=g_A(O_1^2,O_{-1}^2)\ ,\\ &g_{0x}^{(1)}=g_{x0}^{(1)}=g_A(O_1^1,O_{-1}^2)\ ,\\ &g_{\underline{00}}^{(1)}=g_B(O_1^1,O_{-1}^1)\ ,\quad g_{\underline{xx}}^{(1)}=g_B(O_1^2,O_{-1}^2)\ ,\\ &g_{0\underline{x}}^{(1)}=g_{\underline{x}0}^{(1)}=g_B(O_1^1,O_{-1}^2)\ . \end{aligned} \tag{44}$$

For the $T2$ mode, O_Q^1 vertices do not appear. On the other hand, functions like $g(O_2^2,O_2^2)$ and $g(O_{-2}^2,O_{-2}^2)$ occur. We find that Eq. (43) again gives the excitation energies, provided that we replace $A_0^{(p)}$ and $B_0^{(p)}$ by $B_2^{(p)}$ and $A_0^{(a)}$ and $B_0^{(a)}$ by $B_2^{(a)}$, and provided that we write

$$\begin{aligned} &g_{00}^{(2)}=g_A(O_2^2,O_{-2}^2)\ ,\\ &g_{xx}^{(2)}=g_A(O_{-2}^2,O_2^2)\ ,\\ &g_{0x}^{(2)}=g_A(O_2^2,O_2^2)\ ,\\ &g_{x0}^{(2)}=g_A(O_{-2}^2,O_{-2}^2)=g_{0x}^{(2)}\ ,\\ &g_{\underline{00}}^{(2)}=g_B(O_2^2,O_{-2}^2)\ ,\\ &g_{\underline{xx}}^{(2)}=g_B(O_{-2}^2,O_2^2)\ ,\\ &g_{0\underline{x}}^{(2)}=g_B(O_2^2,O_2^2)\ ,\\ &g_{\underline{x}0}^{(2)}=g_B(O_{-2}^2O_{-2}^2)=g_{0\underline{x}}^{(2)}\ . \end{aligned} \tag{45}$$

We note that Eq. (43) for the antiferromagnetic excitation energies is of an order in ω_l that is twice that of Eq. (26) for the ferromagnetic excitation energies. The same is true for the corresponding equations for the $T1$ and $T2$ modes. This tells us that compared to the ferromagnet, the antiferromagnet has twice as many excitation branches in each mode. This effect is expected and is associated with the existence of two sublattices in the case of the antiferromagnet.

VI. DISORDERED PHASE

The equations for the excitation energies simplify in the paramagnetic phase. The simplications are a consequence of time-reversal symmetry and cubic symmetry which exist in the paramagnetic phase.

In the longitudinal case, time-reversal symmetry demands that

$$g_{0x}(\omega_l)=g_{x0}(\omega_l)=0\ . \tag{46}$$

This can be easily demonstrated by remembering that

$$g_{0x}(\omega_l)=\langle T_\tau O_0^1(\tau)O_0^2(0)\rangle_{\omega_l}\ . \tag{47}$$

Under the operation of time reversal the right-hand-side of Eq. (47) becomes $-\langle T_\tau O_0^1(\tau)O_0^2(0)\rangle_{\omega_l}=-g_{0x}(\omega_l)$, which under time-reversal symmetry must be equal to what it was before the time-reversal operation. The only way this can happen is for $g_{0x}(\omega_l)=0$. We have similarly shown that $g_{x0}(\omega_l)=0$ as well.

Using Eq. (46), we find that our equation $D_0^A(\vec{q},\omega_l)=0$ is now factorizable, and becomes

$$D_0^A(\vec{q},\omega)=\{1-(g_{00}+g_{\underline{00}})A_0^{(p)}+g_{00}g_{\underline{00}}[(A_0^{(p)})^2-(A_0^{(a)})^2]\}\{1-(g_{xx}+g_{\underline{xx}})B_0^{(p)}+g_{xx}g_{\underline{xx}}[(B_0^{(p)})^2-(B_0^{(a)})^2]\}\ , \quad (48)$$

which can be further factored as

$$D_0^A(\vec{q},\omega)=[1-g_{00}(A_0^{(p)}+A_0^{(a)})][1-g_{00}(A_0^{(p)}-A_0^{(a)})][1-g_{xx}(B_0^{(p)}+B_0^{(a)})][1-g_{xx}(B_0^{(p)}-B_0^{(a)})]=0\ , \quad (49)$$

after utilizing $g_{00}=g_{\underline{00}}$ and $g_{xx}=g_{\underline{xx}}$ because of the equivalence of the two sublattices. Setting each factor to zero in Eq. (49) yields four sets of solutions.

Equation (49) is very informative because it demonstrates that in the paramagnetic phase, the L mode consists of four types of solutions, two of which are identifiable as magnetic dipolar excitations since they are associated solely with Heisenberg exchange coupling (the A couplings) and two of which are identifiable as quadrupole excitations since they are associated solely with quadrupole couplings (the B couplings). We employ the labels $LD(1)$, $LD(2)$, $LQ(1)$, and $LQ(2)$ as follows:

$$\begin{aligned}
&1-g_{00}(A_0^{(p)}+A_0^{(a)})=0 \quad [LD(1)\text{ mode}]\ ,\\
&1-g_{00}(A_0^{(p)}-A_0^{(a)})=0 \quad [LD(2)\text{ mode}]\ ,\\
&1-g_{xx}(B_0^{(p)}+B_0^{(a)})=0 \quad [LQ(1)\text{ mode}]\ ,\\
&1-g_{xx}(B_0^{(p)}-B_0^{(a)})=0 \quad [LQ(2)\text{ mode}]\ .
\end{aligned} \quad (50)$$

In the transverse $T1$ case, we again have

$$g_{0x}^{(1)}(\omega_l)=g_{x0}^{(1)}(\omega_l)=0\ , \quad (51)$$

where these quantities are defined through Eqs. (44) and (15). Cubic symmetry is responsible for Eq. (51), and the reader should refer to Appendix A for details. Using Eq. (51), we find that

$$\begin{aligned}
D_1^A(\vec{q},\omega_l)=&[1-g_{00}^{(1)}(A_1^{(p)}+A_1^{(a)})]\\
&\times[1-g_{00}^{(1)}(A_1^{(p)}-A_1^{(a)}]\\
&\times[1-g_{xx}^{(1)}(B_1^{(p)}+B_1^{(a)})]\\
&\times[1-g_{xx}^{(1)}(B_1^{(p)}-B_1^{(a)})]=0\ ,
\end{aligned} \quad (52)$$

and we obtain the $T1D(1), T1D(2), T1Q(1), T1Q(2)$ modes as follows:

$$\begin{aligned}
&1-g_{00}^{(1)}(A_1^{(p)}+A_1^{(a)})=0 \quad [T1D(1)]\ ,\\
&1-g_{00}^{(1)}(A_1^{(p)}-A_1^{(a)})=0 \quad [T1D(2)]\ ,\\
&1-g_{xx}^{(1)}(B_1^{(p)}+B_1^{(a)})=0 \quad [T1Q(1)]\ ,\\
&1-g_{xx}^{(1)}(B_1^{(p)}-B_1^{(a)})=0 \quad [T1Q(2)]\ .
\end{aligned} \quad (53)$$

In Appendix A it is demonstrated that as a consequence of cubic symmetry, the $T1D(1)$ and $T1D(2)$ equations have exactly the same solutions as the $LD(1)$ and $LD(2)$ equations given in Eqs. (50).

The transverse $T2$ case is a little more complicated because $g_{0x}^{(2)}$ and $g_{x0}^{(2)}$ are not identically zero in the paramagnetic case. We do have

$$\begin{aligned}
&g_{0x}^{(2)}(\omega_l)=g_{x0}^{(2)}(\omega_l)=g_{0\underline{x}}^{(2)}(\omega_l)=g_{\underline{x}0}^{(2)}(\omega_l)\ ,\\
&g_{00}^{(2)}(\omega_l)=g_{xx}^{(2)}(\omega_l)=g_{0\underline{0}}^{(2)}(\omega_l)=g_{\underline{xx}}^{(2)}(\omega_l)\ ,
\end{aligned} \quad (54)$$

and a result we obtain for the paramagnet the equation

$$\begin{aligned}
D_2^A(\vec{q},\omega_l)=&(1-2g_{00}^{(2)}B_2^{(p)})^2-2(g_{0x}^{(2)})^2[(B_2^{(p)})^2+(B_2^{(a)})^2]+2(g_{00}^{(2)})^2[(B_2^{(p)})^2-(B_2^{(a)})^2]\\
&-4\{[(g_{00}^{(2)})^2-(g_{0x}^{(2)})^2]g_{00}^{(2)}\}[(B_2^{(p)})^2-(B_2^{(a)})^2]B_2^{(p)}+[(g_{00}^{(2)})^2-(g_{0x}^{(2)})^2]^2[(B_2^{(p)})^2-(B_2^{(a)})^2]^2=0\ .
\end{aligned} \quad (55)$$

In Appendix A it is demonstrated that owing to the cubic symmetry this equation may be written as follows:

$$\begin{aligned}
D_2^A(\vec{q},\omega_l)=&[1-g_{00}(B_0^{(p)}+B_0^{(a)})]\\
&\times[1-g_{00}(B_0^{(p)}-B_0^{(a)})]\\
&\times[1-g_{xx}^{(1)}(B_1^{(p)}+B_1^{(a)})]\\
&\times[1-g_{xx}^{(1)}(B_1^{(p)}-B_1^{(a)})]=0\ ,
\end{aligned} \quad (56)$$

where the g_{00} and $g_{xx}^{(1)}$ refer to the appropriate g functions in the longitudinal and $T1$ case. Thus, we see that in the disordered phase we get a set of $T2$ modes corresponding to $LQ(1)$ and $LQ(2)$ and another set of $T2$ modes corresponding to $T1Q(1)$ and $T1Q(2)$.

We now demonstrate, however, that a reciprocal lattice translation can take the $LD(2)$, $LQ(2)$, and $T1Q(2)$ modes into the $LD(1)$, $LQ(1)$, and $T1Q(1)$ modes, respectively. As an example we consider a type-II ordering, although the result should be true for type-I ordering as well.

Referring to the diagram in Fig. 3, one may demonstrate that for type-II ordering

$$\gamma_{nn}^{(p)}(\vec{q}) = \frac{1}{z_{(p)}} \sum_{\langle\vec{\delta}\rangle}^{AA} e^{i\vec{q}\cdot\vec{\delta}} = \frac{1}{3}\left[\cos\frac{a}{2}(q_x - q_y) + \cos\frac{a}{2}(q_x + q_z) + \cos\frac{a}{2}(q_y + q_z)\right]$$

$$\gamma_{nn}^{(a)}(\vec{q}) = \frac{1}{z_{(a)}} \sum_{\langle\vec{\delta}\rangle}^{AB} e^{i\vec{q}\cdot\vec{\delta}} = \frac{1}{3}\left[\cos\frac{a}{2}(q_x + q_y) + \cos\frac{a}{2}(q_x - q_z) + \cos\frac{a}{2}(q_y - q_z)\right]$$

$$\gamma_{nnn}^{(a)}(\vec{q}) = \frac{1}{y_{(a)}} \sum_{\langle\langle\vec{\delta}\rangle\rangle}^{AB} e^{i\vec{q}\cdot\vec{\delta}} = \frac{1}{3}(\cos aq_x + \cos aq_y + \cos aq_z) \quad , \tag{57}$$

where a is the lattice constant. One then finds that

$$\begin{aligned} \gamma_{nn}^{(p)}(\vec{q}+\vec{K}) &= \gamma_{nn}^{(p)}(\vec{q}) \quad , \\ \gamma_{nn}^{(a)}(\vec{q}+\vec{K}) &= -\gamma_{nn}^{(a)}(\vec{q}) \quad , \\ \gamma_{nnn}^{(a)}(\vec{q}+\vec{K}) &= -\gamma_{nnn}^{(a)}(\vec{q}) \quad , \end{aligned} \tag{58}$$

for $\vec{K} = (\pi/a)(1, 1, \bar{1})$. Thus, from Eqs. (39) and (42), $A_Q^{(p)} - A_Q^{(a)}$ goes over to $A_Q^{(p)} + A_Q^{(a)}$ under the reciprocal-lattice translation $\vec{K}$, and similarly $B_Q^{(p)} - B_Q^{(a)}$ goes over to $B_Q^{(p)} + B_Q^{(a)}$.

In our previous paper,[9] in which we analyzed model ferromagnet with nearest-neighbor coupling, we found only modes given by

$$\begin{aligned} 1 - [A_0^{(p)}(\text{nn}) + A_0^{(a)}(\text{nn})]g_{00} &= 0 \quad (LD) \quad , \\ 1 - [B_0^{(p)}(\text{nn}) + B_0^{(a)}(\text{nn})]g_{xx} &= 0 \quad (LQ) \quad , \\ 1 - [B_1^{(p)}(\text{nn}) + B_1^{(a)}(\text{nn})]g_{xx}^{(1)} &= 0 \quad (T1Q) \quad . \end{aligned} \tag{59}$$

The addition of nnn coupling would be expected to alter the dispersion but should not produce additional modes. Indeed, the other solutions $LD(2)$, $LQ(2)$, and $T1Q(2)$ arise simply because of the two-sublattice scheme used in our present calculation.

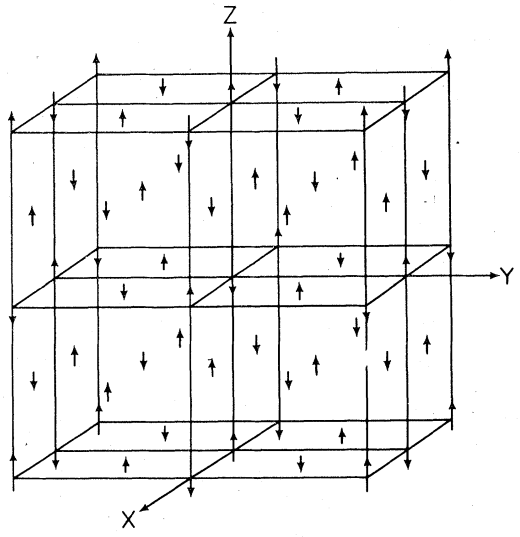

FIG. 3. Diagram showing type-II ordering in an fcc lattice. The $(11\bar{1})$ planes are ferromagnetically ordered within the plane and antiferromagnetically ordered between planes. (After ter Haar and Lines[13]).

They are $LD(1)$, $LQ(1)$, and $T1Q(1)$ solutions transferred from the part of the first Brillouin zone of the full lattice which is severed off in the two-sublattice scheme. Hereafter we shall ignore the $LD(2)$, $LQ(2)$, and $T1Q(2)$ solutions and label the remaining solutions as LD, LQ, and $T1Q$.

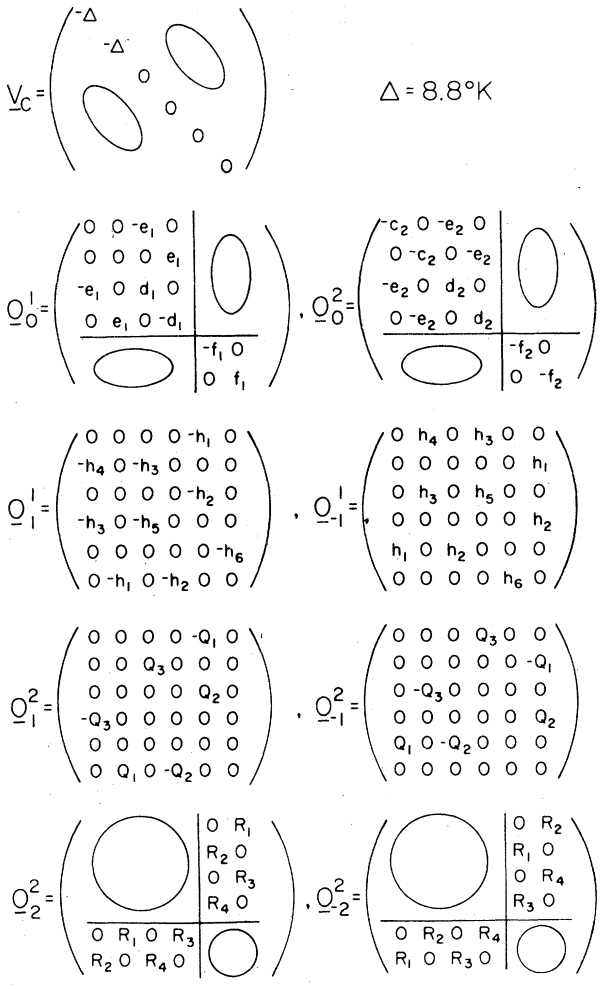

FIG. 4. Matrices for various operators evaluated with respect to cubic crystal-field states for DySb. A six-level scheme is used.

VII. APPLICATION TO DySb

DySb is one of the systems which have definitive evidences of quadrupolar coupling.[7,12,23] It is type-II antiferromagnetic at low temperatures and the discontinuous phase transition at 9.5 °K is accompanied by a slight tetragonal distortion of the lattice.[24] The discontinuous phase transition behavior is attributed to the presence of quadrupolar coupling between ions.

In DySb, the cubic crystal field splits the 16-fold degenerate free-ion ground-state energy level into 5 levels: Γ_6, $\Gamma_8^{(1)}$, Γ_7, $\Gamma_8^{(2)}$, and $\Gamma_8^{(3)}$. The ground state, Γ_6, is a Kramer's doublet. The most recent scheme suggested for the other levels by Kouvel *et al.*[12] is $\Gamma_8^{(1)}$ at 8.8 °K, Γ_7 at 60.4 °K, $\Gamma_8^{(2)}$ at 96.0 °K, and $\Gamma_8^{(3)}$ at 120.2 °K. The crystal-field coefficients[15] we shall use are $A_4\langle r^4\rangle = 60$ °K and $A_6\langle r^6\rangle = 1.8$ °K, consistent with those suggested by Kouvel *et al.*[12]

Since the ordering temperature is 9.5 °K, if the temperature is not too much higher than the ordering temperature, it is reasonable to approximate the system by a two-level scheme consisting of Γ_6 and $\Gamma_8^{(1)}$. The form of the appropriate crystal field matrix elements is shown in Fig. 4.

In order to solve for the single-ion basis states used for the unperturbed Green's functions in type-II antiferromagnetic DySb we use the mean-field Hamiltonian from Eq. (4). This Hamiltonian may be rewritten

$$H_0 = H_A + H_B = \sum_i^A \{V_c(i,A) - [\lambda_1' M_A + (\lambda_1+\lambda_3) M_B] O_0^1(i,A) - [\lambda_2' Q_A + (\lambda_2+\lambda_4) Q_B] O_0^2(i,A)\}$$
$$+ \sum_i^B \{V_c(i,B) - [\lambda_1' M_B + (\lambda_1+\lambda_3) M_A] O_0^1(i,B) - [\lambda_2' Q_B + (\lambda_2+\lambda_4) Q_A] O_0^2(i,B)\} , \quad (60)$$

where

$$M_A = \langle O_0^1(A)\rangle , \quad M_B = \langle O_0^1(B)\rangle ,$$
$$Q_A = \langle O_0^2(A)\rangle ,$$

and

$$Q_B = \langle O_0^2(B)\rangle ,$$

and where the definition of the coupling energies λ_i should be clear from comparing Eq. (4) with Eq. (60). Using the crystal-field matrices given in Fig. 4, matrices for $\underline{H}_A$ and $\underline{H}_B$ are then formed from Eq. (60). These matrices are then diagonalized and eigenenergies $\{E_n^A\}$ and $\{E_n^B\}$ are obtained for sites on the A sublattice and B sublattice, respectively. The eigenvectors associated with the diagonalized $\underline{H}_A$ and $\underline{H}_B$ give the molecular-field state functions for sublattices A and B. The molecular-field energies and state functions depend on the values of M_A, M_B, Q_A, and Q_B, which are determined self-consistently as a function of temperature from the relations

$$M_A = \frac{1}{Z_A}\sum_n e^{-\beta E_n^{(A)}}\left(-\frac{1}{\lambda_1+\lambda_3}\frac{\partial E_n^{(A)}}{\partial M_B}\right) ,$$
$$M_B = \frac{1}{Z_B}\sum_n e^{-\beta E_n^{(B)}}\left(-\frac{1}{\lambda_1+\lambda_3}\frac{\partial E_n^{(B)}}{\partial M_A}\right) ,$$
$$Q_A = \frac{1}{Z_A}\sum_n e^{-\beta E_n^{(A)}}\left(-\frac{1}{\lambda_2+\lambda_4}\frac{\partial E_n^{(A)}}{\partial Q_B}\right) ,$$
$$Q_B = \frac{1}{Z_B}\sum_n e^{-\beta E_n^{(B)}}\left(-\frac{1}{\lambda_2+\lambda_4}\frac{\partial E_n^{(B)}}{\partial Q_A}\right) . \quad (61)$$

Here Z_A and Z_B represent the single-ion partition functions for sublattices A and B, respectively.

The choice of λ_i determines the ordering temperature T_N. Since in the antiferromagnetic phase, $M_A = -M_B$ and $Q_A = Q_B$, we find that H_0 reduces to

$$H_0 = \sum_i^A [V_c(i,A) - \lambda_3 M_B O_0^1(i,A) - (2\lambda_2+\lambda_4) \times Q_B O_0^2(i,A)] + \sum_i^B [V_c(i,B) - \lambda_3 M_A O_0^1(i,B) - (2\lambda_2+\lambda_4) Q_A O_0^2(i,B)] , \quad (62)$$

if we choose $\lambda_1' = \lambda_1$ and $\lambda_2' = \lambda_2$, assuming thus that nn parallel spins are coupled with the same strength as nn antiparallel spins. We choose $\lambda_3 = -0.40$ °K and $2\lambda_2 + \lambda_4 = 0.001$ °K in order to produce a discontinuous phase transition at $T_N = 9.52$ °K, the experimental transition temperature quoted by Bucher *et al.*[7] In addition, this choice yields a saturation sublattice magnetization $M_{sat} = 9.75\mu_B$ and a ratio $|M_A|/M_{sat} = 86.7\%$ at $T = 9.0$ °K, also in excellent agreement with the experimental values.[25]

Our fit to T_N does not let us determine λ_1. This we determine from the paramagnetic Curie temperature θ, using the relation[14]

$$\theta = \frac{2J(J+1)}{3k_B}(6\hat{J}_{(p)} + 6\hat{J}_{(a)} + 6\hat{I}_{(a)})$$
$$= \frac{2J(J+1)}{3k_B}\left(\lambda_1 + \frac{\lambda_3}{2}\right) , \quad (63)$$

where J for Dy^{3+} is $\frac{15}{2}$. Busch *et al.*[26] have found θ equal to -4 °K. This yields $\lambda_1 = \lambda_1' = +0.106$ °K. This is reasonable since we expect the exchange coupling to exhibit an RKKY range behavior,[27] and it is therefore not surprising that the nn coupling has a sign opposite to that of the nnn coupling.

We note that in Eq. (63) we have neglected the effect of quadrupolar coupling on the paramagnetic Curie temperature. This can be justified. Following an earlier work by Wang[28] we show that the shift in θ by the quadrupolar couplings is given by

$$\Delta\theta = -\frac{J(J+1)}{3k_B}\left(\lambda_2 + \frac{\lambda_4}{2}\right) . \tag{64}$$

The derivation is given in Appendix B. Since $\lambda_2 + \frac{1}{2}\lambda_4$ is more than two orders of magnitude smaller than $\lambda_1 + \frac{1}{2}\lambda_3$, the correction $\Delta\theta$ can be neglected.

Still undetermined are λ_2, λ_2', and λ_4. We have so far only that $\lambda_2 + \lambda_2' + \lambda_4 = 0.001$ °K. In the absence of any other information, we choose $\lambda_2 = \lambda_2' = \lambda_4 = \frac{1}{3}(0.001)$ °K. Comparison with experimental neutron data on the DySb excitation energies would give better grounds for a choice. Hopefully this paper might serve to stimulate such measurements.

Excitation energies in the ordered phase may be determined by solving Eq. (43) numerically. A computer program has been constructed to do this using the Newton-Raphson method[29] to search for the roots. The program is general enough that it may be used for any rare-earth system whose molecular-field states are describable by the two-sublattice model. All that has to be supplied is the molecular-field states. The program has been used also to reconstruct the excitation modes for the nn ferromagnet model and gives agreement with the program which uses Eqs. (26), (28), and (31) as a basis for computation.

In the disordered phase, we can obtain analytic solutions for the excitation energies from Eqs. (50) and (52). Using the matrix elements e_1, e_2, Q_1, and Q_3 shown in Fig. 4 to evaluate the g functions, we obtain

$$\begin{aligned}
\epsilon_{\vec{q}}^{(LD)} &= \{\Delta^2 - 4[a_0^{(p)}(\vec{q}) + a_0^{(a)}(\vec{q})](e_1)^2 D_{13}\Delta\}^{1/2} = \epsilon_{\vec{q}}^{(T1D)} \\
\epsilon_{\vec{q}}^{(LQ)} &= \{\Delta^2 - 4[b_0^{(p)}(\vec{q}) + b_0^{(a)}(\vec{q})](e_2)^2 D_{13}\Delta\}^{1/2} = \epsilon_{\vec{q}}^{(T2_1)} \\
\epsilon_{\vec{q}}^{(T1Q)} &= \{\Delta^2 + 2[b_1^{(p)}(\vec{q}) + b_1^{(a)}(\vec{q})][(Q_1)^2 + (Q_3)^2] D_{13}\Delta\}^{1/2} = \epsilon_{\vec{q}}^{(T2_2)}
\end{aligned} \tag{65}$$

where

$$a_Q^{(p)} = A_Q^{(p)}/\beta , \quad a_Q^{(a)} = A_Q^{(a)}/\beta ,$$
$$b_Q^{(p)} = B_Q^{(p)}/\beta , \text{ and } b_Q^{(a)} = B_Q^{(a)}/\beta ,$$

and where

$$D_{13} = (e^{\beta\Delta} - 1)/(2e^{\beta\Delta} + 4) . \tag{66}$$

We shall display the results for the DySb excitation energies in Sec. VIII.

VIII. DISCUSSION

Figures 5–10 show the excitation energies for DySb for $\vec{q}$ equal to $q(1,0,0)$, $q(1,1,1)$, $q(0,1,1)$, and $q(1,1,\bar{1})$. These $\vec{q}$ are all in special directions. From Fig. 3 we see that the $(11\bar{1})$ planes are ferromagnetic planes. An excitation with $\vec{q} = q(0,1,1)$ propagates within such planes, whereas an excitation with $\vec{q} = q(1,1,\bar{1})$ propagates perpendicular to such planes. Excitations with $\vec{q} = q(1,0,0)$ and $\vec{q} = q(1,1,1)$ propagate in high symmetry directions in the full Brillouin zone. Of all these special directions only the $\langle 1,1,\bar{1}\rangle$ direction has a Brillouin-zone boundary that is different for the sublattice (see Appendix C).

We observe the following general characteristics in Figs. 5–10. Above the ordering temperature, the LD, LQ, and $T1Q$ modes have one branch only.[30] The dispersion of the LD and LQ modes is appreciable and comparable to that found with the nn ferromagnet model used in our earlier paper.[9] We note that a different crystal-field level structure was used in Ref. (9), with Δ equal to 14.5 °K instead of 8.8 °K used here, so the modes there are centered about energies that are shifted from those shown in this paper. The dispersion seen here is also much more complicated owing to the inclusion of nnn coupling. In general, the various modes do not show a monotonic increase with q as in the nn ferromagnet model.

To understand the dispersion behavior of the various modes, we compute $A_0^{(p)}(\vec{q})$, $A_0^{(a)}(\vec{q})$, $B_0^{(p)}(\vec{q})$, and $B_0^{(a)}(\vec{q})$, which enter into Eq. (43). These are plotted in Fig. 11. We remind the reader that the A functions are associated with Heisenberg exchange coupling and the B functions with biquadratic coupling, as seen in Eq. (42).

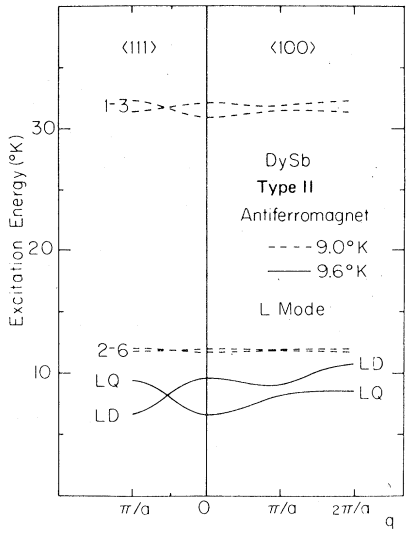

FIG. 5. DySb excitation energies in the longitudinal L mode as a function of $q(1,0,0)$ and $q(1,1,1)$.

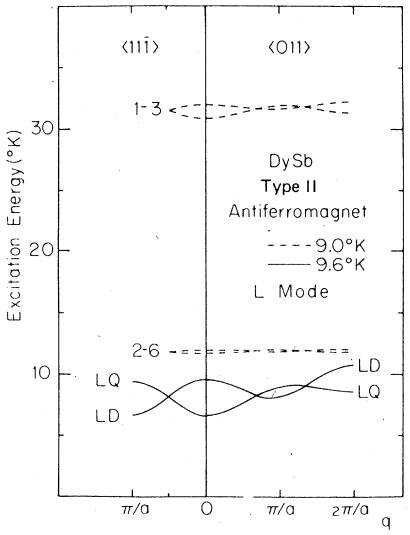

FIG. 6. DySb excitation energies in the longitudinal L mode as a function of $q(0,1,1)$ and $q(1,1,\bar{1})$.

We now examine the dispersion in detail. The LD mode first decreases and then increases with q. The initial decrease is due to antiferromagnetic nnn exchange coupling dominating the behavior at small q. At larger q the competition between ferromagnetic nn coupling and antiferromagnetic nnn coupling is much more complicated and depends on the detailed nature of the various $\gamma(\vec{q})$, which are tabulated for the various $\vec{q}$ directions in Table I.

The LQ mode at first increases with q because all the quadrupolar couplings are ferroquadrupolar. We also note that the LQ mode has value $\epsilon_q^{(LQ)} = \Delta$ at often quite rational values of q. This occurs, for example, at $q = \frac{2}{3}(\pi/a)$ in the $\langle 1,1,\bar{1}\rangle$ direction and again at $q = \frac{2}{3}(\pi/a)$ in the $\langle 1,1,1\rangle$ direction. This happenstance is accidental and is due to the choice that $\lambda_2 = \lambda_2' = \lambda_4$. For example, at $\frac{2}{3}(\pi/a)(1,1,1)$,

$$\gamma_{nn}^{(p)}(q) = 1 \ , \quad \gamma_{nn}^{(a)}(q) = -\tfrac{1}{2} \ , \quad \gamma_{nnn}^{(a)}(q) = -\tfrac{1}{2} \ ,$$

and so $A_Q^{(p)} + A_Q^{(a)} = 0$ and $\epsilon_q^{(LQ)} = \Delta$ if $\lambda_2 = \lambda_2' = \lambda_4$. It should also be noted that although the biquadratic

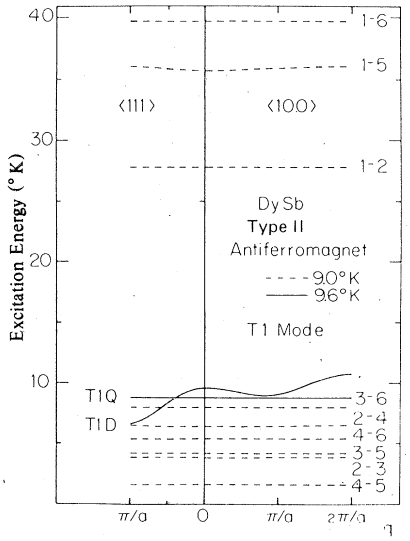

FIG. 7. DySb excitation energies in the transverse $T1$ mode as a function of $q(1,0,0)$ and $q(1,1,1)$.

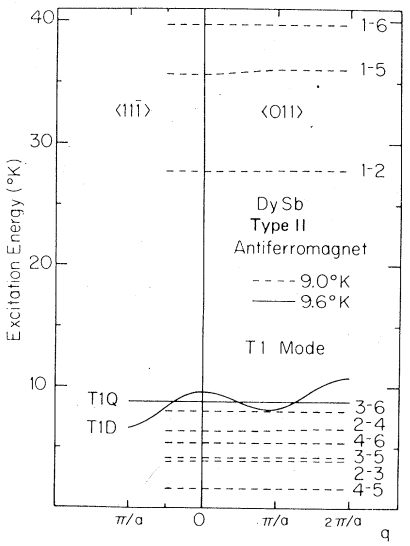

FIG. 8. DySb excitation energies in the transverse $T1$ mode as a function of $q(0,1,1)$ and $q(1,1,\bar{1})$.

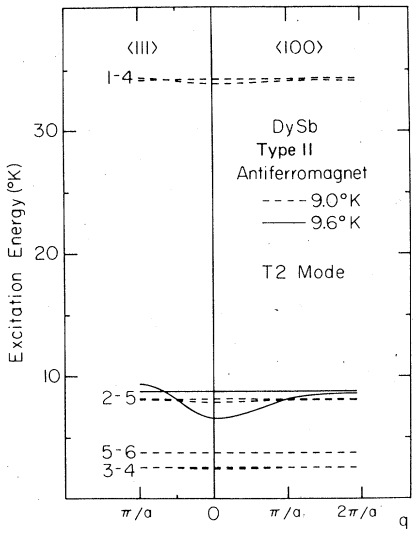

FIG. 9. DySb excitation energies in the transverse $T2$ mode as a function of $q(1,0,0)$ and $q(1,1,1)$.

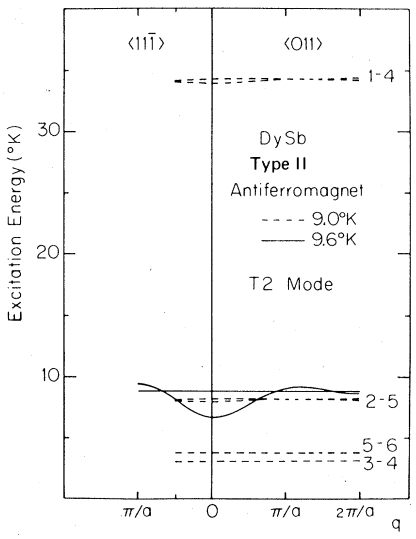

FIG. 10. DySb excitation energies in the transverse $T2$ mode as a function of $q(0,1,1)$ and $q(1,1,\bar{1})$.

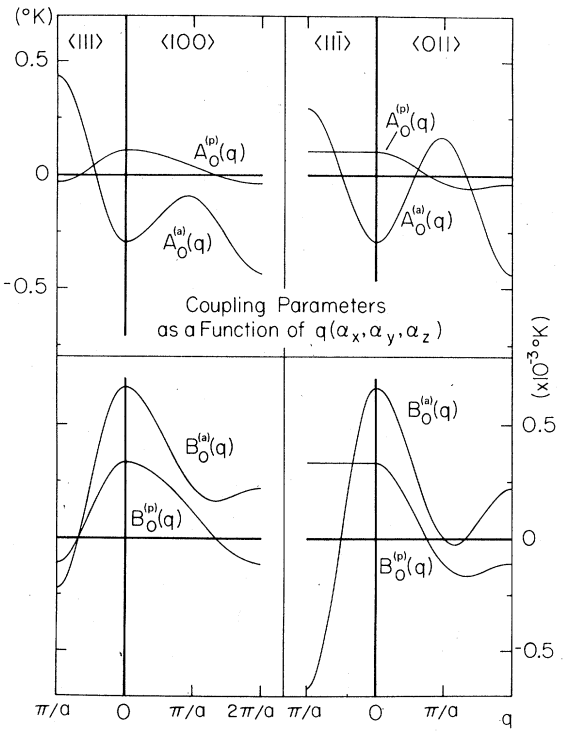

FIG. 11. Functions $A_0^{(p)}(\vec{q})$, $A_0^{(a)}(\vec{q})$, $B_0^{(p)}(\vec{q})$, and $B_0^{(a)}(\vec{q})$ as functions of $\vec{q}$ for the directions $\langle 1,0,0\rangle$, $\langle 1,1,1\rangle$, $\langle 0,1,1\rangle$, and $\langle 1,1,\bar{1}\rangle$.

TABLE I. Functions $\gamma(\vec{q})$ for various directions of $\vec{q}$.

$q = q\langle 1,0,0\rangle$	
	$\gamma_{nn}^{(p)}(\vec{q}) = \frac{1}{3}\left[2\cos\left(\frac{aq}{2}\right)+1\right]$
	$\gamma_{nn}^{(a)}(\vec{q}) = \frac{1}{3}\left[2\cos\left(\frac{aq}{2}\right)+1\right]$
	$\gamma_{nnn}^{(a)}(\vec{q}) = \frac{1}{3}(\cos aq + 2)$
$q = q\langle 1,1,1\rangle$	
	$\gamma_{nn}^{(p)}(\vec{q}) = \frac{1}{3}(1 + 2\cos aq)$
	$\gamma_{nn}^{(a)}(\vec{q}) = \frac{1}{3}(2 + \cos aq)$
	$\gamma_{nnn}^{(a)}(\vec{q}) = \cos aq$
$q = q\langle 0,1,1\rangle$	
	$\gamma_{nn}^{(p)}(\vec{q}) = \frac{1}{3}\left[2\cos\left(\frac{aq}{2}\right)+\cos aq\right]$
	$\gamma_{nn}^{(a)}(\vec{q}) = \left[2\cos\left(\frac{aq}{2}\right)+1\right]$
	$\gamma_{nnn}^{(a)}(\vec{q}) = \frac{1}{3}(2\cos aq + 1)$
$q = q\langle 1,1,\bar{1}\rangle$	
	$\gamma_{nn}^{(p)}(\vec{q}) = 1$
	$\gamma_{nn}^{(a)}(\vec{q}) = \cos aq$
	$\gamma_{nnn}^{(a)}(\vec{q}) = \cos aq$

coupling energies are much smaller than the exchange energies, the square of the matrix element of O_0^2 is about 400 times larger than that of O_0^1, and hence the LQ mode has a dispersion comparable to that of the LD. The $T1Q$ mode is flat because in this case the $O_{\pm1}^2$ quadrupolar transition matrix elements responsible for it are much smaller than those for O_0^2.

Our plots also confirm that the $T1D$ and the two paramagnetic $T2$ modes have the same energy spectrum as the LD, LQ, and $T1Q$ modes, respectively.

We should like to emphasize that the LQ and $T1Q$ modes are decoupled from the magnetic dipolar excitations. The LQ and $T1Q$ modes are pure quadrupolar modes and arise as a direct result of quadrupolar coupling. All cubic systems that exhibit quadrupolar coupling should have such modes. The temperature behavior of LD modes has been observed in neutron inelastic scattering experiments for compounds with bilinear only coupling in a crystal field.[20] It would be of great interest to observe the pure quadrupolar LQ modes in similar experiments. The fact that $\Delta m = 0$ (no spin flip) has the greatest intensity in neutron-scattering measurements[31] also makes the observation of the LQ mode more plausible.

In the ordered phase, the molecular field lifts completely the degeneracy of energy levels. We label the energy levels in numerals in ascending order (1 being the ground level). We note that because of the large energy splittings even near the phase transition, only the ground level is appreciably populated. Therefore only excitations from the ground level and level 2 show any noticeable dispersion.

The chief difference between the antiferromagnet and ferromagnet model in the ordered phase is a doubling of the number of branches in each mode. In the L mode, the antiferromagnet has four branches, whereas the ferromagnet had two. In the $T2$ mode the antiferromagnet has eight branches, whereas the ferromagnet had four. (Not all the eight branches are distinctly shown in our plot because some of the branches are not sufficiently separated.) The $T1$ mode is a different story. The antiferromagnet appears to have the same number of branches as the ferromagnet. However, each of the branches in the antiferromagnet is doubly degenerate. This can be understood if we recall that the antiferromagnet system consists of two sublattices whose wave functions are related by a time-reversal operation in the absence of an external field. The energy associated with spin-raising excitation operators ($\Delta m = +1$) therefore equals that associated with the spin-lowering excitation operators ($\Delta m = -1$). That is, there are two distinct modes of the same energy.

In all cases, the ordered phase excitations are mixed magnetic dipolar and quadrupolar excitations and the varied shapes of the ordered phase dispersion curves show clear evidence of this mixing.

IX. CONCLUSION AND SUMMARY

Inasmuch as biquadratic coupling is an important element in some rare-earth systems, we have devised a Green's-function method which allows one to compute excitation energies in a crystal-field system with bilinear and biquadratic couplings. We have applied the method to a type-II antiferromagnet because we wished to treat a particular system, DySb, which shows strong evidences of biquadratic coupling.

We have found in general that there are three types of modes: a longitudinal ($\Delta m = 0$) mode (L mode) associated with O_0^1 and O_0^2 operators, a transverse ($\Delta m = \pm 1$) mode ($T1$ mode) associated with $O_{\pm1}^1$ and $O_{\pm1}^2$ operators, and a transverse ($\Delta m = 2$) mode ($T2$ mode) associated with $O_{\pm2}^2$ operators. In the ordered phase the L-mode and $T1$-mode excitations are mixed magnetic dipolar and quadrupolar excitations. In the disordered phase the magnetic dipolar modes decouple from the quadrupolar modes, giving rise to the possibility of observing a pure quadrupolar excitation in the L- and $T1$-modes.

The dispersion in the type-II antiferromagnet is more complicated than in the nn ferromagnet because of the competing coupling between nearest-neighbor parallel spins, nearest-neighbor antiparallel spins, and next-nearest-neighbor antiparallel spins. There is also a doubling of the number of branches in each mode in the antiferromagnet owing to the halving of the Brillouin zone brought about by the formation of sublattices.

ACKNOWLEDGMENTS

One of us (M.S.) thanks Florida State University for the hospitality extended to him during his several visits. We also thank J. S. Kouvel, P. M. Levy, L. F. Uffer, M. Kalos, K. Rauchwarger, and S. Jafarey for helpful discussions. This work was supported by Research Corporation (M.S.) and the NSF (Y.L.W.).

APPENDIX A: EFFECTS OF CUBIC SYMMETRY ON THE EXCITATION ENERGIES IN THE DISORDERED STATE

We give three proofs here.

1. $g_{0x}^{(1)} = g_{x0}^{(1)} = 0$ *as a consequence of cubic symmetry*

This is important to show because it is the condition which decouples the dipole modes from the quadrupolar modes in the $T1$ case.

We shall use the notation $g_{x0}^{(1)} = \langle O_1^2 \,|\, O_{-1}^1 \rangle$ and $g_{0x}^{(1)} = \langle O_1^1 \,|\, O_{-1}^2 \rangle$.

Consider $\langle (J^x J^z + J^z J^x) \,|\, J^y \rangle$, where the J^x, J^y, J^z are

components of angular-momentum operators. Under a 90° rotation about the y axis, $J^z \rightarrow J^x$ and $J^x \rightarrow -J^z$, and

$$\langle (J^xJ^z + J^zJ^x)|J^y\rangle \rightarrow -\langle (J^zJ^x + J^xJ^z)|J^y\rangle \ .$$

But in cubic symmetry, a quantity such as the above should be invariant under a 90° rotation. The only way a 90° rotation can produce the negative of the quantity is for the quantity to be identically zero. Now, we have

$$O = \langle (J^xJ^z + J^zJ^x)|J^y\rangle$$
$$= \frac{1}{4i}[\langle (J^-J^z + J^zJ^-)|J^+\rangle - \langle (J^+J^z + J^zJ^+)|J^-\rangle$$
$$+ \langle (J^+J^z + J^zJ^+)|J^+\rangle - \langle (J^-J^z + J^zJ^-)|J^-\rangle] \ .$$

The last two terms are zero because two raising operations or two lowering operations cannot connect cubic crystal-field states. Call the first two terms A and B.

Now consider $\langle (J^xJ^z + J^zJ^x)|J^x\rangle$ and take it through a 180° rotation about the y axis, so that $J^x \rightarrow -J^x$ and $J^z \rightarrow -J^z$. It follows that

$$\langle (J^xJ^z + J^zJ^x)|J^x\rangle \rightarrow -\langle (J^xJ^z + J^zJ^x)|J^x\rangle \ ,$$

and hence we have

$$O = \langle (J^xJ^z + J^zJ^x)J^x\rangle$$
$$= \frac{1}{4i}[\langle (J^+J^z + J^zJ^+)|J^-\rangle + \langle (J^-J^z + J^zJ^-)|J^+\rangle] \ .$$

We have shown in effect that $A - B = 0$ and $A + B = 0$ so that A and B are separately zero, and hence that

$$\langle (J^+J^z + J^zJ^+)|J^-\rangle = \langle (J^-J^z + J^zJ^-)|J^+\rangle = 0 \ ,$$

which is equivalent to saying that

$$g_{0x}^{(1)} = g_{x0}^{(1)} = 0 \ . \ \text{Q.E.D.}$$

2. *LD mode has the same solutions as the T1D, as a consequence of cubic symmetry.*

We need to show that

$$1 - g_{00}(A_0^{(p)} + A_0^{(a)}) = 1 - g_{00}^{(1)}(A_1^{(p)} + A_1^{(a)}) \ . \quad \text{(A1)}$$

This is equivalent to showing that

$$\langle J^z|J^z\rangle(A_0^{(p)} + A_0^{(a)}) = \tfrac{1}{2}\langle J^+|J^-\rangle(A_0^{(p)} + A_0^{(a)}) \ , \quad \text{(A2)}$$

where we have used $A_1^{(p)} = -A_0^{(p)}$, $A_1^{(a)} = -A_0^{(a)}$, $O_1^1 = -(\frac{1}{2})^{1/2}J^+$ and $O_{-1}^1 = (\frac{1}{2})^{1/2}J^-$. But

$$\langle J^+|J^-\rangle = \langle J^x|J^x\rangle + \langle J^y|J^y\rangle + i(\langle J^y|J^x\rangle - \langle J^x|J^y\rangle) \ .$$

Under a 90° rotation about the z axis, the term in the parentheses becomes the negative of itself and hence, under cubic symmetry, must vanish. The remaining terms are equal to $2\langle J^z|J^z\rangle$ since x, y, and z are equivalent under cubic symmetry. Q.E.D.

3. *T2 modes have solutions which correspond to LQ and T1Q modes, as a consequence of cubic symmetry*

We wish to show that

$$[1 - 2\langle O_0^2|O_0^2\rangle B_{(p)} + \langle O_0^2|O_0^2\rangle^2(B_{(p)}^2 - B_{(a)}^2)][1 + 2\langle O_1^2|O_{-1}^2\rangle B_{(p)} + \langle O_1^2|O_{-1}^2\rangle^2(B_{(p)}^2 - B_{(a)}^2)]$$
$$= (1 - 2\langle O_2^2|O_{-2}^2\rangle B_{(p)})^2 - 2\langle O_2^2|O_2^2\rangle^2(B_{(p)}^2 + B_{(a)}^2)) + 2\langle O_2^2|O_{-2}^2\rangle^2(B_{(p)}^2 - B_{(a)}^2)$$
$$- 4\langle O_2^2|O_{-2}^2\rangle(\langle O_2^2|O_{-2}^2\rangle^2 - \langle O_2^2|O_2^2\rangle^2)B_{(p)}(B_{(p)}^2 - B_{(a)}^2) + (\langle O_2^2|O_{-2}^2\rangle^2$$
$$- \langle O_2^2|O_2^2\rangle^2)^2(B_{(p)}^2 - B_{(a)}^2)^2 \ , \quad \text{(A3)}$$

where the first factor on the left-hand side (set equal to zero) gives the solutions for the LQ modes, the second factor (set equal to zero) gives the solutions for the $T1Q$ modes, and where the right-hand side represents $D_2^A(\vec{q}, \omega)$. Note that we have used $B_0^{(p)} = -B_1^{(p)} = B_2^{(p)} \equiv B_{(p)}$ and $B_0^{(a)} = -B_1^{(a)} = B_2^{(a)} \equiv B_{(a)}$.

From Eqs. (3) defining the spherical tensor operators, we have that

$$\langle O_0^2|O_0^2\rangle = \tfrac{3}{4}\langle J^{x2} - J^{y2}|J^{x2} - J^{y2}\rangle \ ,$$
$$\langle O_1^2|O_{-1}^2\rangle = -\tfrac{3}{4}\langle J^xJ^y + J^yJ^x|J^xJ^y + J^yJ^x\rangle \ ,$$
$$\langle O_2^2|O_{-2}^2\rangle = \tfrac{3}{8}\langle J^{x2} - J^{y2}|J^{x2} - J^{y2}\rangle$$
$$+ \tfrac{3}{8}\langle J^xJ^y + J^yJ^x|J^xJ^y + J^yJ^x\rangle$$
$$+ i\tfrac{3}{8}(\langle J^xJ^y + J^yJ^x|J^{x2} - J^{y2}\rangle$$
$$- \langle J^{x2} - J^{y2}|J^xJ^y + J^yJ^x\rangle) \ . \quad \text{(A4)}$$

A rotation of 180° about the x axis takes $J^x \rightarrow J^x$, $J^y \rightarrow -J^y$, and $J^z \rightarrow -J^z$ while leaving the above quantities invariant. This requires that

$$\langle J^xJ^y|J^{x2}\rangle = -\langle J^xJ^y|J^{x2}\rangle = 0 \ ,$$
$$\langle J^xJ^y|J^{y2}\rangle = -\langle J^xJ^y|J^{y2}\rangle = 0 \ ,$$
$$\langle J^yJ^x|J^{x2}\rangle = -\langle J^yJ^x|J^{x2}\rangle = 0 \ ,$$
$$\langle J^yJ^x|J^{y2}\rangle = -\langle J^yJ^x|J^{y2}\rangle = 0 \ ,$$

so that in cubic symmetry

$$\langle O_0^2|O_0^2\rangle = \tfrac{3}{4}\langle (J^x)^2 - (J^y)^2|(J^x)^2 - (J^y)^2\rangle \ ,$$
$$\langle O_1^2|O_{-1}^2\rangle = -\tfrac{3}{4}\langle J^xJ^y + J^yJ^x|J^xJ^y + J^yJ^x\rangle \ ,$$
$$\langle O_2^2|O_{-2}^2\rangle = \tfrac{3}{8}\langle (J^x)^2 - (J^y)^2|(J^x)^2 - (J^y)^2\rangle$$
$$+ \tfrac{3}{8}\langle J^xJ^y + J^yJ^x|J^xJ^y + J^yJ^x\rangle \ . \quad \text{(A5)}$$

These are all real and

$$\langle O_0^2 | O_0^2 \rangle - \langle O_1^2 | O_{-1}^2 \rangle = 2 \langle O_2^2 | O_{-2}^2 \rangle \ . \tag{A6}$$

We can also show that

$$\langle O_2^2 | O_2^2 \rangle = \tfrac{3}{8} \langle (J^x)^2 - (J^y)^2 | (J^x)^2 - (J^y)^2 \rangle - \tfrac{3}{8} \langle J^x J^y + J^y J^x | J^x J^y + J^y J^x \rangle \ ,$$

and hence that

$$\langle O_2^2 | O_{-2}^2 \rangle^2 - \langle O_2^2 | O_2^2 \rangle^2 = - \langle O_0^2 | O_0^2 \rangle \langle O_1^2 | O_{-2}^2 \rangle \ . \tag{A7}$$

Using Eqs. (A6) and (A7), one can then demonstrate that Eq. (A3) is an equality. The algebra is left to the reader. Q.E.D.

APPENDIX B: DERIVATION OF THE BILINEAR AND BIQUADRATIC CONTRIBUTIONS TO THE PARAMAGNETIC CURIE TEMPERATURE

We here give an expanded version of the development used in the letter by Wang.[28]

Let the Hamiltonian of the system be $\mathcal{H}$ and the measuring field be $\vec{H}$. Since we are interested in the linear response of the system to the perturbing field $\vec{H}$, we need to calculate its effects on the wave functions only to first order. Let $|n\rangle$ be a complete set of eigenfunctions of $\mathcal{H}$,

$$\mathcal{H} |n\rangle = E_n |n\rangle \ .$$

Choose $\vec{H}$ along the z axis. To first order of H, the perturbed states and energies are

$$|\tilde{n}\rangle = |n\rangle - h \sum_{\substack{m \\ m \neq n}}{}' \frac{\langle m | \sum_i J_i^z | n \rangle}{E_n - E_m} |m\rangle \tag{B1}$$

and

$$\tilde{E}_n = E_n - h \langle n | \sum_i J_i^z | n \rangle \ , \tag{B2}$$

where $h = g_J \mu_B H$ and g_J is the Landé g factor.

The induced magnetization is

$$\delta M = g_J \mu_B \delta \langle \sum_i J_i^z \rangle \ ,$$

where

$$\delta \langle \sum_i J_i^z \rangle = \sum_n \langle \tilde{n} | \sum_i J_i^z | \tilde{n} \rangle e^{-\beta \tilde{E}_n} \Big/ \sum_n e^{-\beta \tilde{E}_n} - \sum_n \langle n | \sum_i J_i^z | n \rangle e^{-\beta E_n} \Big/ \sum_n e^{-\beta E_n} \ , \tag{B3}$$

where we have taken the volume of the sample as unity.

The susceptibility is defined as

$$\chi = \lim_{H \to 0} \frac{\delta M}{H} \ ,$$

and we obtain

$$(g_J \mu_B)^{-2} \chi = \frac{1}{Z} \beta \sum_n \langle n | \sum_i J_i^z | n \rangle^2 e^{-\beta E_n} - \frac{1}{Z^2} \beta \left(\sum_n \langle n | \sum_i J_i^z | n \rangle e^{-\beta E_n} \right)^2 + \frac{1}{Z} \sum_{\substack{n,m \\ n \neq m}}{}' \frac{2 | \langle m | \sum_i J_i^z | n \rangle |^2}{E_m - E_n} e^{-\beta E_n} \ , \tag{B4}$$

where $Z = \sum_n e^{-\beta E_n}$.

At high temperatures (viz., $k_B T$ much greater than the total energy splitting of the ground multiplet), we expand χ as a power series of β,

$$(g_J \mu_B)^{-2} \chi = C_0 + C_1 \beta + C_2 \beta^2 + C_3 \beta^3 + \cdots \ , \tag{B5}$$

where

$$C_0 = \frac{2}{Z} \sum_{\substack{n,m \\ n \neq m}}{}' \frac{| \langle m | \sum_i J_i^z | n \rangle |^2}{E_m - E_n} = 0 \ ,$$

$$C_1 = (2J+1)^{-N} \sum_n \langle n | \left(\sum_i J_i^z \right)^2 | n \rangle = \tfrac{1}{3} N J (J+1) \ ,$$

$$C_2 = -(2J+1)^{-N} \sum_n \left[\langle n | \left(\sum_i J_i^z \right)^2 | n \rangle - \tfrac{1}{3} N J (J+1) \right] E_n \ . \tag{B6}$$

The higher-order coefficients can be found similarly, but we need to know only C_1 and C_2 for the expression of θ. We expand χ^{-1} in β and obtain

$$(g_J \mu_B)^2 \chi^{-1} = \frac{1}{C_1 \beta} - \frac{C_2}{C_1^2} - \frac{1}{C_1^3} (C_1 C_3 + C_2^2) \beta + \cdots \ . \tag{B7}$$

Thus a plot of χ^{-1} vs T will show a straight line at high temperature and the intercept θ_z of the extrapolation of this line to the T axis is $C_2/(C_1 k_B)$. So we have

$$k_B \theta_z = C_2 / C_1 \ . \tag{B8}$$

After writing C_2 and C_1 in trace form, we have

$$k_B \theta_z = -\mathrm{Tr} \left\{ \left[\left(\sum_i J_i^z \right)^2 - N J (J+1)/3 \right] \mathcal{H} \right\} \Big/ \mathrm{Tr} \left(\sum_i J_i^z \right)^2 \ . \tag{B9}$$

For a measuring field in the x and y directions we replace z by x or y in the above expression. The powder average is

$$k_B\theta = -\frac{1}{3}\,\mathrm{Tr}\left[\left(\sum_{\substack{i,j\\ i\neq j}} \vec{\mathfrak{J}}_i\cdot\vec{\mathfrak{J}}_j\right)\mathfrak{K}\right] \Big/ \mathrm{Tr}\left(\sum_i J_i^z\right)^2 \quad . \tag{B10}$$

To evaluate θ, we first note that

$$\mathrm{Tr}(J_1^z)^2 = \sum_{\substack{n_1 n_2 \cdots\\ =-J}}^{J} \langle n_1 n_2 \cdots | (J_1^z)^2 | n_1 n_2 \cdots \rangle = (2J+1)^{N-1} \sum_{n_1=-J}^{J} n_1^2 = \tfrac{1}{3}J(J+1)(2J+1)^N \quad ,$$

and hence the denominator of our expression for θ is $(\frac{1}{3}N)J(J+1)(2J+1)^N$. The numerator depends on the Hamiltonian $\mathfrak{K}$.

If $\mathfrak{K} = -\sum_{l,m}\hat{J}_{lm}\vec{J}_l\cdot\vec{J}_m$, which is the bilinear exchange term, then the numerator is

$$\mathrm{Tr}\left[\left(\sum_{\substack{i,j\\ i\neq j}} (J_i^x J_j^x + J_i^y J_j^y + J_i^z J_j^z)\right) \times \left(-\sum_{l,m}\hat{J}_{lm}(J_l^x J_m^x + J_l^y J_m^y + J_l^z J_m^z)\right)\right] = -2\times 3\,\mathrm{Tr}\sum_{l,m}\hat{J}_{lm}(J_l^x)^2(J_m^x)^2 \quad ,$$

where we drop all terms with zero trace and where the factor of 2 comes from the two ways of obtaining nonzero contribution, namely (i) $i=l$, $j=m$ and (ii) $i=m, j=l$. Writing

$$N\hat{J}(0) = \sum_{\substack{l,m\\ l\neq m}} \hat{J}_{lm} \quad ,$$

and using the tables of Ambler *et al.*,[32] we find that the numerator is $-\frac{2}{3}N\hat{J}(0)(2J+1)^N J^2(J+1)^2$ and hence that

$$k_B\theta_m = \tfrac{2}{3}\hat{J}(0)J(J+1) \quad . \tag{B11}$$

For an fcc crystal with nn and nnn coupling, this becomes

$$k_B\theta_m = \tfrac{2}{3}J(J+1)[\tfrac{1}{2}(\lambda_1+\lambda_1'+\lambda_3)]$$

if we use the notation in the text of this paper.

We can obtain the effect of biquadratic exchange by setting $\mathfrak{K} = -\sum_{l,m}\hat{K}_{lm}(\vec{J}_l\cdot\vec{J}_m)^2$. The numerator in Eq. (A17) then becomes

$$-3\times 2\times 2\,\mathrm{Tr}\left(\sum_{lm}\hat{K}_{lm}J_l^x J_l^y J_l^z J_m^x J_m^y J_m^z\right) = (N/3)\hat{K}(0)(2J+1)^N J^2(J+1)^2 \quad ,$$

where again we have explicitly dropped all the terms with zero trace, and where again we use the tables of Ambler *et al.*[32] This gives as the biquadratic correction to the paramagnetic Curie temperature

$$k_B\theta_q = -\tfrac{1}{3}\hat{K}(0)J(J+1) \quad . \tag{B12}$$

$$\mathrm{Tr}\left(\sum_i J_i^z\right)^2 = \mathrm{Tr}\left[\sum_i (J_i^z)^2 + \sum_{\substack{i,j\\ i\neq j}} J_i^z J_j^z\right] \quad .$$

The second term is zero. For the first term we have

We note that Eq. (B10) is so constructed that each term in $\mathfrak{K}$ gives a contribution to θ and all the contributions add together, so

$$k_B\theta = k_B(\theta_m+\theta_q) = \tfrac{2}{3}\hat{J}(0)J(J+1) - \tfrac{1}{3}\hat{K}(0)J(J+1) \quad . \tag{B13}$$

Normally $\hat{K}(0)$ is much smaller than $\hat{J}(0)$, and hence the second term is not a large correction.

Also, as shown by Wang,[28] the cubic crystal-field term in the Hamiltonian does not alter θ and hence Eq. (B13) has all the corrections in it that we need to consider for this paper.

APPENDIX C: SUBLATTICE BASIS VECTORS, RECIPROCAL-LATTICE VECTORS, AND BRILLOUIN-ZONE BOUNDARIES IN THE TYPE-II ANTIFERROMAGNET

Sublattice points are given by $(1,1,\bar{1})$ ferromagnetic sheets. Such points are generated by the primitive vectors

$$\begin{aligned} \vec{a}_1 &= (\tfrac{1}{2}a)\hat{i} + (\tfrac{1}{2}a)\hat{k} \quad ,\\ \vec{a}_2 &= (\tfrac{1}{2}a)\hat{j} + (\tfrac{1}{2}a)\hat{k} \quad ,\\ \vec{a}_3 &= -a\hat{i} + a\hat{k} \quad , \end{aligned} \tag{C1}$$

where a is the lattice constant of the fcc lattice, and where the X-Y-Z axes used are those of Fig. 3. The sublattice is triclinic. The volume occupied by the sublattice is

$$\vec{a}_1\times\vec{a}_2\cdot\vec{a}_3 = \tfrac{1}{2}a^3 \quad .$$

The primitive vectors in the reciprocal lattice are

$$\begin{aligned} \vec{b}_1 &= 2\pi\left(\frac{2}{a^3}\vec{a}_2\times\vec{a}_3\right) = \frac{2\pi}{a}(\hat{i}-\hat{j}+\hat{k}) \quad ,\\ \vec{b}_2 &= 2\pi\left(\frac{2}{a^3}\vec{a}_3\times\vec{a}_1\right) = \frac{2\pi}{a}(2\hat{j}) \quad ,\\ \vec{b}_3 &= 2\pi\left(\frac{2}{a^3}\vec{a}_1\times\vec{a}_2\right) = \frac{2\pi}{a}(-\tfrac{1}{2}\hat{i}-\tfrac{1}{2}\hat{j}+\tfrac{1}{2}\hat{k}) \quad . \end{aligned} \tag{C2}$$

We find first Brillouin-zone boundaries in various directions as follows. In the $\langle 1,1,\bar{1}\rangle$ direction we find the zone boundary by showing first that $(\pi/a)(1,1,\bar{1})$ is a reciprocal lattice vector. This is true if we have

$$(\pi/a)(\hat{i}+\hat{j}-\hat{k}) = m_1\vec{b}_1 + m_2\vec{b}_2 + m_3\vec{b}_3 \ ,$$

where the m_i are integers. The equation is satisfied by $m_1=0$, $m_2=0$, $m_3=-1$. The first Brillouin-zone boundary is halfway along this vector at $(\pi/2a)(1,1,\bar{1})$. In a similar way we show that the Brillouin-zone boundary in the $\langle 1,1,1\rangle$ direction is at $(\pi/a)(1,1,1)$, in the $\langle 0,1,1\rangle$ direction is at $(2\pi/a)(0,1,1)$, and in the $\langle 1,0,0\rangle$ direction is at $(2\pi/a)(1,0,0)$.

[1]F. Keffer, in *Handbuch der Physik,* edited by S. Flügge (Springer-Verlag, New York, 1966), Vol. XVIII/2, p. 1.

[2]Yu. A. Izyumov and R. P. Ozerov, *Magnetic Neutron Diffraction* (Plenum, New York, 1970).

[3]A. R. Mackintosh and H. B. Møller, in *Magnetic Properties of Rare Earth Metals,* edited by R. J. Elliott (Plenum, New York, 1972), p. 187.

[4]See, for example, B. R. Cooper, in *Magnetic Properties of Rare Earth Metals,* edited by R. J. Elliott (Plenum, New York, 1972), p. 17.

[5]M. Blume and Y. Hsieh, J. Appl. Phys. 40, 1249 (1968); J. Sivardiere and M. Blume, Phys. Rev. B 5, 1126 (1972); H. H. Chen and P. M. Levy, Phys. Rev. B 7, 4267 (1973).

[6]M. Barma, Phys. Rev. B 10, 4650 (1974); I. P. Fittipaldi and R. A. Tahir-Kheli, Phys. Rev. B 12, 1839 (1975); S. T. Chiu-Tsao, P. M. Levy, and C. Paulson, Phys. Rev. B 12, 1819 (1975); S. T. Chiu-Tsao and P. M. Levy, Phys. Rev. B 13, 3046 (1976); B. Westwanski, Acta Pol. Phys. A 47, 777 (1975); K. Skrobis and B. Westwanski, Physica (Utrecht) 83 A, 257 (1976); R. Micnas, Phys. Status Solidi B 72, 255 (1975); J. Phys. C 9, 3307 (1976).

[7]E. Bucher, R. J. Birgeneau, J. P. Maita, G. P. Felcher, and T. O. Brun, Phys. Rev. Lett. 28, 746 (1972).

[8]G. A. Gehring and K. A. Gehring, Rep. Prog. Phys. 38, 1 (1975); J. Sivardiere, J. Magn. Matter 1, 183 (1976).

[9]M. Sablik and Y. L. Wang, J. Appl. Phys. 49, 1419 (1977).

[10]For example, dhcp Pr, B. D. Rainford and J. G. Houmann, Phys. Rev. Lett. 26, 1254 (1971).

[11]For example, Pr_3Tl, J. Als-Nielsen, W. J. Buyers, J. K. Kjems, and R. J. Birgeneau, Proc. Int. Conf. Magn. 1976, 1162 (1977).

[12]G. P. Felcher, T. O. Brun, R. J. Gambino, and M. Kuznietz, Phys. Rev. B 8, 260 (1973); T. J. Moran, R. L. Thomas, P. M. Levy, and H. H. Chen, Phys. Rev. B 7, 3238 (1973); P. M. Levy, M. J. Sablik, H. Taub, L. F. Uffer, and S. J. Williamson, Proc. Int. Conf. Magnetism 1973 (Nauka, Moscow, 1974), Vol. 6, p. 217; T. O. Brun, G. H. Lander, F. W. Korty, and J. S. Kouvel, AIP Conf. Proc. 24, 244 (1974); P. Streit, G. E. Everett, and A. W. Lawson, Phys. Lett. 60A, 199 (1974); J. S. Kouvel, T. O. Brun, and F. W. Korty, Physica (Utrecht) 86-88B, 1043 (1977).

[13]D. ter Haar and M. E. Lines, Phil. Trans. R. Soc. London, Ser. A 255, 1049 (1962).

[14]J. S. Smart, *Effective Field Theories of Magnetism* (Saunders, Philadelphia, 1966), Ch. 8.

[15]K. R. Lea, M. J. M. Leask, and W. P. Wolf, J. Phys. Chem. Solids 23, 1381 (1962).

[16]A. Abragam and B. Bleaney, *Electron Paramagnetic Resonance of Transition Ions* (Oxford, London, 1970), p. 863.

[17]A. A. Abrikosov, L. P. Gorkov, and I. Ye. Dzyaloshinskii, *Quantum Field Theoretical Methods in Statistical Physics,* (Pergamon, New York, 1965), Ch. 3.

[18]S. B. Haley and P. Erdös, Phys. Rev. B 5, 1106 (1972).

[19]D. H. Yang and Y. L. Wang, Phys. Rev. B 10, 4714 (1974); 12, 1057 (1975).

[20]W. J. L. Buyers, T. M. Holden, and A. Perreault, Phys. Rev. B 11, 266 (1975).

[21]J. M. Robinson, AIP Conf. Proc. 34, 189 (1976); S. B. Haley, Phys. Rev. B 17, 338 (1978).

[22]Y. L. Wang, S. Shtrikman, and H. Callen, Phys. Rev. 144, 419 (1966).

[23]P. M. Levy, J. Phys. C 6, 3545 (1973).

[24]F. Levy, Phys. Konden. Mater. 10, 85 (1969).

[25]L. F. Uffer, P. M. Levy, and H. H. Chen, AIP Conf. Proc. 10, 553 (1973).

[26]G. Busch, O. Marincek, A. Menth, and O. Vogt, Phys. Lett. 14, 262 (1965).

[27]H. H. Teitelbaum and P. M. Levy, Phys. Rev. B 14, 3058 (1976).

[28]Y. L. Wang, Phys. Lett. A 35, 383 (1971).

[29]D. D. McCracken and W. S. Dorn, *Numerical Methods and Fortran Programming* (Wiley, New York, 1968), p. 133.

[30]Our computations on HoSb, for example, indicate that the *LD* mode has two branches in HoSb if a six-level scheme is used. In both HoSb and DySb there ought to be more branches than that if more than six levels are included in the crystal-field scheme.

[31]P. M. Levy and G. T. Trammell, J. Phys. C 10, 1303 (1977).

[32]E. Ambler, J. C. Eisenstein, and J. F. Schooley, J. Math. Phys. (N.Y.) 3, 118 (1962).